University of Texas at El Paso
DigitalCommons@UTEP

Open Access Theses & Dissertations

2017-01-01

Evaluation Of Cryptic Sulfur Cycling In Marine Sediments

Michael Ngari Mathuri
University of Texas at El Paso, mykmathuri@gmail.com

Follow this and additional works at: https://digitalcommons.utep.edu/open_etd

 Part of the Geochemistry Commons

Recommended Citation
Mathuri, Michael Ngari, "Evaluation Of Cryptic Sulfur Cycling In Marine Sediments" (2017). *Open Access Theses & Dissertations*. 499.
https://digitalcommons.utep.edu/open_etd/499

This is brought to you for free and open access by DigitalCommons@UTEP. It has been accepted for inclusion in Open Access Theses & Dissertations by an authorized administrator of DigitalCommons@UTEP. For more information, please contact lweber@utep.edu.

EVALUATION OF CRYPTIC SULFUR CYCLING IN MARINE SEDIMENTS

MICHAEL NGARI MATHURI

Master's Program in Geological Sciences

APPROVED:

Benjamin Brunner, Ph.D., Chair

Gail Lee Arnold, Ph.D.

Virgil Lueth, Ph.D.

Charles Ambler, Ph.D.
Dean of the Graduate School

Copyright ©

by

Michael Ngari Mathuri

2017

DEDICATION

This thesis is dedicated to my loving girlfriend Wincate Karimi,

my mother Esther Muthoni Mathuri and my sister Joyce Wanjiku.

Your words of encouragement and urge for tenacity ring in my mind and ears.

EVALUATION OF CRYPTIC SULFUR CYCLING IN MARINE SEDIMENTS

by

MICHAEL NGARI MATHURI, B.S.

THESIS

Presented to the Faculty of the Graduate School of
The University of Texas at El Paso
in Partial Fulfillment
of the Requirements
for the Degree of

MASTER OF SCIENCE

Department of Geological Sciences
THE UNIVERSITY OF TEXAS AT EL PASO
May 2017

ACKNOWLEDGEMENTS

I would first like to sincerely thank my thesis advisor Dr. Benjamin Brunner from the Department of Geological Sciences at the University of Texas at El Paso for his continuous support and motivation during my Master's study. The door to Dr. Brunner's office was always open whenever I had a question about my research or writing. He consistently allowed this research to be my own work, but steered me in the right direction whenever he thought I needed it. Besides research, Dr. Brunner was also very concerned about my later career as a scientist. He was always happy to discuss with me the many possible job opportunities in the world of Isotope Biogeochemistry.

I would also like to thank other members of my thesis committee: Dr. Virgil Lueth and Dr. Gail Lee Arnold for their encouragement and insightful comments. Without their passionate participation and input, this research work could not have been successfully conducted. My sincere thanks also go to Jeff Baker, a student at the University of Texas at El Paso and a professional glass blower. Jeff was the brain behind the production of isotope label glass ampules used in my sediment incubation experiments.

Finally, I must express my profound gratitude to my lab colleague Marisela Montelongo for providing me with unfailing support in the lab and continuous encouragement throughout the process of research and writing this thesis. This accomplishment would not have been possible without you. Thank you Shela.

ABSTRACT

Despite the importance of marine sediments as a carbon sink and many efforts to integrate microbiological with geochemical and geological data, the understanding of microbial organic carbon mineralization processes in marine sediments remains incomplete. There is growing evidence for the existence of an unrecognized oxidative sulfur cycling (cryptic sulfur cycling) above, within and below of the main sulfate reduction zone. For example, sulfate exists in supposedly sulfate-free methanogenic marine sediments from the Aarhus Bay and Black Sea. This implies that sulfur cycling is an ongoing process in the deep biosphere. Quantification of cryptic sulfur cycling is a major challenge because it does not leave an imprint in the net sulfur budget of the surrounding environment.

My goal is to quantify cryptic sulfur cycling in sediments and assess if it is of significant importance to organic carbon mineralization. Sediment samples for my project were collected from the Kattegat-Skagerrak region located in Danish, Norwegian and Swedish national waters. With these sediment samples, I conducted sediment incubation studies in airtight bags fitted with Rhizon® samplers to allow non-destructive sampling of pore-water at different points of time.

I developed experimental protocols that allow for the monitoring of cryptic sulfur cycling with the help of $^{34}S_{SO4}$ and $^{18}O_{H2O}$ labels that were released from ampules embedded in sediment incubations, which were kept strictly anaerobic. My incubation experiments resulted in the surprising finding that once sulfate is introduced, sulfate reduction rates are extremely high, and that the rate of oxygen isotope exchange between sulfate and water mediated by sulfate reducing microbes was similar to pure culture incubations. Apparently, during the long storage of the sediments, the sulfate-reducing microbes ran out of sulfate, and were limited to the supply from sulfate from oxidative processes, fueled by oxygen that diffused into the storage bags. This relative

lack of sulfate as central terminal electron acceptor led to the accumulation of organic substrates that are favorable for sulfate reducing microbes. Once sulfate was supplied, sulfate reduction immediately proceeded at astonishingly high rates. Thus, my incubation experiments cannot be considered to be representative for cryptic sulfur cycling in marine sediments. Nevertheless, I make key observations that can contribute to the body of research on cryptic sulfur cycling. The initial concentration of sulfate in the bags was approximately 37µM, a value that is similar to what has been postulated as sulfate concentrations below the sulfate methane transition. Apparently, even the high availability of organic substrates for the sulfate reducing microbes in the storage bags did not allow sulfate-reducing organisms to lower the sulfate concentration even further. This implies that there is a link between sulfate concentrations, and energetic threshold for dissimilatory sulfate reduction. Finally, inhibition of sulfate reduction with the help of molybdate reveals that sulfate consumption continues to proceed at low rates, however, with very little associated oxygen isotope exchange between sulfate and water. Potentially, inhibition with molybdate alters the sulfate reduction pathway in a manner where the process becomes less reversible. This possibility offers a new avenue to study the mechanisms of stepwise sulfate reduction by or dissimilatory sulfate bacteria. Alternatively, the decline in sulfate concentrations could be attributed to assimilatory processes. If this is the case, the slow increase in the oxygen isotope composition of sulfate would represent the elusive fingerprint of cryptic sulfur oxidation.

TABLE OF CONTENTS

LIST OF TABLES

LIST OF FIGURES

1. INTRODUCTION

Sulfur is an element commonly occurring in nature. Sulfur compounds such as sulfate and sulfide play important roles in redox processes as electron acceptor or donor, connecting the sulfur cycle with other major biogeochemical element cycles, such as the carbon or nitrogen cycle. Despite extensive studies (Canfield et al., 2010; Holmkvist, Kamyshny Jr., et al., 2011; Jasińska et al., 2012; Deusner et al., 2014; Scheller et al., 2016), questions concerning how sulfur cycling operates in marine sediments remain unresolved. There is growing evidence for the existence of hidden oxidative sulfur cycling (cryptic sulfur cycling) above, within and below of the main sulfate reduction zone. For example, sulfate reducing organisms have been found below the sulfate-methane transition in supposedly sulfate-free methanogenic marine sediments from the Aarhus Bay and Black Sea (Leloup et al., 2007; Leloup et al., 2009) and sulfate exists below the sulfate-methane transition in Aarhus Bay (Holmkvist, Ferdelman, et al., 2011). This occurrence of sulfate implies that sulfide gets oxidized back to sulfate in the methanogenic zone, which is not predicted thermodynamically.

The above observations touch upon the fundamental principle in biogeochemistry that different groups of microorganisms carrying out different processes are confined to different environments (Figure 1). The presence of sulfate reducers in the methanogenic zone does not comply with this concept because it demonstrates that different organisms can thrive outside of the classical zone in the marine redox tower attributed to their metabolism. This is not impossible, because as long as organisms can gain energy by employing alternative pathways, they may thrive in a redox zone that is classically assigned to another main metabolic process. Moreover, recently, it was suggested that sulfate reduction coupled to the anaerobic oxidation of methane might employ a sulfate reduction pathway that yields zero-valent sulfur that is subsequently disproportionated into sulfate

and sulfide (Milucka et al., 2012) – a process that would constitute a hidden cycle on its own, allowing for extensive sulfur oxidation in an environment that drives sulfate reduction.

1.1 IMPORTANCE OF CRYPTIC SULFUR CYCLING

For two reasons, studying cryptic sulfur cycling is important.

1) The existence of redox reactions outside of their commonly assigned redox zone indicates that the classical principle of a redox tower may be an inaccurate description of the processes that truly occur in marine sediments. Information that supports this hypothesis could induce a paradigm shift, i.e. break up or weaken the principle of compartmentalized redox zones in favor of an alternative concept that integrates reactions that at first sight appear to be inconceivable because they operate against a thermodynamic gradient.

2) The process of sulfate reduction has been monitored using the ^{35}S-radiotracer technique where ^{35}S-sulfate gets reduced to form ^{35}S-sulfide. Oxidation of sulfide back to sulfate hardly transfers any ^{35}S-sulfide back to the sulfate. This is because the existing sulfide pool largely dilutes the produced ^{35}S-sulfide. In presence of oxidative sulfur cycling, sulfate reduction rates determined by the ^{35}S-radiotracer method would exceed the net sulfate reduction rates calculated from the analysis of pore-water sulfate. Existence of such a hidden process would therefore lead to overestimation of the rates of sulfate removal from the pore-water. Estimates of sulfate reduction based on the study of sulfate concentration profiles – which provide accurate rates of sulfate removal – on the other hand would tend to underestimate sulfate reduction rates. For the study of the carbon and sulfur cycle in marine sediments both rates must be known, because mineralization rates of organic matter are tied to sulfate reduction

whereas the sulfur budget is tied to actual sulfate removal. If cryptic sulfur cycling is important, sulfate reduction and sulfate removal rates can no longer be treated as equal.

1.2 CHALLENGES IN DETECTING CRYPTIC SULFUR CYCLING AND PURPOSE OF STUDY

While there is a clear need to elucidate cryptic sulfur cycling there is also a massive challenge in doing so. To date, the processes involved in cryptic sulfur cycling are inferred from geochemical and isotope patterns but have never been directly observed or quantified. The difficulty in quantifying cryptic sulfur cycling lies in the fact that this process does not leave an imprint in the net sulfur budget of the surrounding environment. My goal was to overcome this challenge by using laboratory experiments that allow me to quantify cryptic sulfur cycling. The purpose of this study was to carry out well controlled incubation experiments with isotope labels that for the first time pin down and quantify oxidative sulfur cycling in various marine sediments. The projects build on the insight that while sulfur isotope labels cannot show such cryptic sulfur cycling, it can be revealed by oxygen isotope labeling techniques. This is because oxidative and reductive sulfur cycling lead to oxygen transfer between sulfate and water (Brunner et al., 2012; Müller et al., 2013).

1.3 OBJECTIVES

The project had four interconnected objectives:

a) Production of isotopically labeled sulfate ($^{34}S_{SO4}$)

Typically, to determine sulfate reduction rates, commercially available radioactive $^{35}S_{SO4}$ is used. However, for the purpose of carrying out long-term experiments because of the extremely slow sulfate reduction rates in the deep biosphere, the relatively short half-life of ^{35}S (87.2 days) can become a limiting factor. Also, radioactive tracers are a health and safety concern with regards to

the handling of the samples, i.e. pyrolysis of a ^{35}S-labeled sample for oxygen isotope analysis could cause contamination issues. For these reasons, it is advisable to use a stable isotope label instead of ^{35}S. There is commercially available ^{34}S, however, it is in the form of native sulfur, and not as $^{34}S_{SO4}$. Therefore, a method to quantitatively convert native sulfur into sulfate needed to be developed.

b) Establish an incubation technique that excludes artifacts caused by contamination with oxidants, in particular atmospheric oxygen

Probably the most critical point in assessing cryptic sulfur cycling is to be able to rule out that the observed production of sulfate is caused by an artifact, such as the introduction of trace amounts of oxygen from the atmosphere. Anaerobic chambers with oxygen sensors partially resolve this issue, however, care must be taken when labels are introduced into samples. Moreover, such chambers may not be available, which is the case for most sea-going expeditions, during which the marine mud for the experiments is retrieved. Therefore, a technically simple alternative to anaerobic chambers would be of great benefit.

c) Development of a numerical model that can be used in the design of the incubation experiments, as well as in the interpretation of the obtained experimental results

For the planning of the experiments, estimates for the amount of sediment, isotope labels, and duration of the incubations are needed. To obtain such estimates, it was necessary to establish a numerical simulation of cryptic sulfur cycling that allowed to predict isotope trends, and thereby provided the information on the key parameters for the experiment design.

d) Carry out incubation experiments and interpret outcomes with respect to cryptic sulfur cycling

After achieving the first three objectives, incubation experiments to assess cryptic sulfur cycling were carried out.

2. MATERIALS AND METHODS

2.1 SAMPLING LOCATIONS

Sediment samples for my research were obtained during a cruise in the Skagerrak-Kattegat-Belt area located in Danish, Norwegian and Swedish national waters (Figure 2). The six selected sites exhibit strong differences with respect to water depth, sedimentation rate, metal content, sulfate penetration depth, depth of bioirrigation, and Holocene sedimentation history. Therefore, the collected samples allow studying cryptic sulfur cycling processes for a wide range of environmental parameters. Sediments for my research project were collected on September 1, 2014 from station 5 (N 56° 45', E 11° 56') in the Kattegat-Skagerrak belt of the Baltic Sea. These samples were obtained from 0 - 30cm sediment within the main sulfate zone.

2.2 SEDIMENT SAMPLING

Sediments were collected on-board for subsequent shore-based laboratory experiments. Sub-samples for sediment collection for incubation experiments were sampled in nitrogen flushed glove-bag. Sediment samples collected for shore-based laboratory experiments were sealed in gas-tight plastic bags and refrigerated. The sediments were then shipped at 4 to 9 ºC in large, sealed, airtight bags by airfreight to the University of Texas at El Paso (UTEP) where they were stored at room temperature. Incubation experiments were conducted at room temperature. For discussion of impact of different temperature see section 2.6.

2.3 PREPARATION OF ISOTOPICALLY LABELED SULFATE

To produce ^{34}S-labeled sulfate, I obtained native sulfur, which was heavily enriched in ^{34}S (99%). I then oxidized the sulfur to sulfate with the help of bromine, to produce an acidic solution as shown in the reaction below.

$S\ (s) + 3Br_2\ (l) + 4H_2O\ (l) \longrightarrow SO_4^{2-}\ (aq) + 8H^+\ (aq) + 6Br^-\ (aq)$. Chem. Eq. 1

To achieve this goal, ^{34}S-native sulfur crystals were ground into a fine powder using a mortar. The small grain size was expected to enhance the rate of sulfur oxidation by increasing the surface area for the reaction. I weighed 0.0507g of sulfur into a glass serum bottle, added 2ml of deionized water and 1.5ml of liquid bromine (Br_2). Liquid bromine evaporates readily at room temperature - to minimize this loss the serum bottle was capped using a 20mm crimp-top aluminum seal with a gray septa made of butyl rubber that is covered with a film of Teflon (PTFE). This was done in the fume hood to prevent exposure to toxic bromine fumes. The mortar was cleaned by first grinding Kimwipes, and then grinding of sand.

The oxidation of native sulfur with bromine is extremely slow at ambient temperature, but – analogous to oxidation of native sulfur with oxygen (Habashi and Bauer, 1966) – is rapid at temperatures above 120 ^oC (notably, the melting point of sulfur is 115 ^oC). The serum bottle was placed in a 250ml beaker containing about 40ml of deionized water, and the beaker was covered with an aluminum foil. The beaker and its contents were autoclaved at 128 ^oC for 2 hours. The autoclave was allowed to cool down to room temperature before removing the beaker. Unfortunately, the cap did not fully prevent escape of bromine from the serum bottle, and was partially damaged during the procedure. This bromine reacted with the aluminum seal, as well as with the aluminum foil that covered the beaker, likely forming aluminum (III) bromide ($AlBr_3$) according to the reaction below:

$2Al\ (s) + 3Br_2\ (l) \longrightarrow 2AlBr_3\ (s)$. Chem. Eq. 2

Aluminum (III) bromide is a highly hygroscopic compound at standard conditions. It absorbs moisture or water to form aluminum hydroxide ($Al(OH)_3$), a white solid, and hydrogen bromide in the reaction:

$AlBr_3$ (s) + $3H_2O$ (l) ⟶ $Al(OH)_3$ (s) + 3HBr (g) . Chem. Eq. 3

The white solids of aluminum hydroxide were found at the neck of the bottle. I washed off the solids with deionized water. To expel any excess bromine, the red-brown solution was boiled in a three-armed glass flask for about 10 minutes inside the fume hood. The resulting solution was yellow in color and contained sulfate and bromide ions. The absence of bromine was tested by using pH indicator paper. If bromine is present, the paper is bleached.

After cooling, the solution was filtered through a 0.45μm membrane syringe filter to remove any suspended solids and then neutralized using sodium hydroxide. White gels, supposedly aluminum hydroxide, formed at a pH of around 7. It is very likely that this was contamination from the degradation of the aluminum caps during the oxidation of sulfur with bromine. Aluminum hydroxide is amphoteric. It dissolves in acid, forming aluminum hydroxide complexes ($[Al(H_2O)_6]^{3+}$), according to

$Al(OH)_3$ (s) + $3H_2O$ (l) + $3H^+$ (aq) ⟶ $[Al(H_2O)_6]^{3+}$ (aq) . Chem. Eq. 4

These soluble aluminum hydroxide complexes precipitate as aluminum hydroxide at neutral pH, according to

$[Al(H_2O)_6]^{3+}$ (aq) + $3OH^-$ (aq) ⟶ $Al(OH)_3$ (s) + $6H_2O$ (l) . Chem. Eq. 5

These white precipitates were then filtered off using 0.45μm membrane syringe filters to obtain a clear ^{34}S-labeled sulfate solution.

2.4 PREPARATION OF GLASS AMPULES CONTAINING ISOTOPICALLY LABELED SOLUTIONS

The isotopically labeled solutions were held in two serum bottles. The first bottle contained 12.5ml solution made by mixing 5ml of 0.037M ^{34}S-labeled sulfate with 7.5ml of ^{18}O-labeled water (98% ^{18}O). The second bottle contained 4.5ml solution for the control experiment. This was prepared by mixing 1ml of 0.037M ^{34}S-labeled sulfate, 1.5ml of ^{18}O-labeled water and 2ml of 1.25M sodium

molybdate. Both bottles were tightly capped using 20mm gray butyl rubber stoppers and crimp-top aluminum seals.

The isotope labels were released into the incubation bags by cracking glass ampules that were placed in the bag together with the sediment. These ampules were produced in-house with help of Jeff Baker, a professional glass blower who is a student at the University of Texas at El Paso. The technique involved specialized equipment that utilizes oxygen enriched propane fire. Six borosilicate glass tubes were heated to temperatures of about 820 ºC and pulled to thicknesses of approximately 0.5mm. One of the open ends of each glass tube was closed and allowed to cool at room temperature prior to addition of the labeled solutions.

As the glass tubes cooled, the serum bottles containing the labeled solutions were prepared for flushing with argon gas. This involved fitting two gas lines to the rubber stopper of each serum bottle, one as an inlet for argon gas and the other as an outlet. The inlet line was dipped into the solutions. Argon gas was bubbled through the solutions for about 10 minutes to drive off any dissolved oxygen. Using a 10ml syringe fitted with a needle, 4.5ml was drawn from 12.5ml solution into each of the five glass tubes. 4.5ml of the control solution was drawn from the bottle into the sixth glass tube. Argon gas was continuously blown into the tubes while adding the solutions to minimize the risk of contamination with atmospheric oxygen. It is presumed that the argon gas (mass 40), which is denser than oxygen (mass 32) and nitrogen (mass 28) displaces the air from the tubes. The tubes were then closed and allowed to cool at room temperature, producing six airtight glass ampules, each approximately 6cm long. A future improvement of this procedure could be achieved by using additional oxygen scrubbing approaches, such as inline scavenging with heated iron or copper filings, to remove oxygen from the argon gas.

2.5 PREPARATION OF ASCORBIC ACID SOLUTION (OXYGEN SCRUBBER)

To keep my experiments strictly anaerobic, I made use of the fact that ascorbic acid ($C_6H_8O_6$) is an antioxidant, and therefore an oxygen scavenger. I used this reagent to maintain anaerobic conditions in the container in which the sediment incubations were placed. At typical biological pH conditions, ascorbate ($C_6H_7O_6$) is the most predominant species of ascorbic acid. In presence of an oxidant (such as oxygen), ascorbate is consumed in a reaction that forms dehydroascorbic acid ($C_6H_6O_6$), according to the reaction below.

$$2C_6H_7O_6\ (aq) + 0.5O_2\ (g) \longrightarrow 2C_6H_6O_6\ (aq) + H_2O\ (l)\ .$$ Chem. Eq. 6

Resazurin was used as redox indicator. In absence of oxygen (i.e. under reducing conditions) Resuazurin is colorless, whereas it becomes pink under oxygenated conditions. Reszurin also acts as a pH indicator, at low pH it turns pink, which could be misinterpreted as oxic conditions. Consequently, it is of great importance to maintain neutral conditions in sediment incubation experiments. To achieve this, calcium carbonate, which acts as a buffer, can be added to ascorbic acid to form calcium ascorbate solution as described in the following reaction:

$$2C_6H_8O_6\ (aq) + CaCO_3\ (s) \longrightarrow C_{12}H_{14}CaO_{12}\ (aq) + CO_2\ (g) + H_2O\ (l)\ .$$ Chem. Eq. 7

To prepare the calcium ascorbate solution, at least 8g of calcium carbonate was added into 2000ml media bottles, which were subsequently filled with deionized water. The mixture was brought to a boil while bubbling with nitrogen gas to drive out dissolved oxygen. The boiling solutions were transferred into three 1-gallon glass pickle jars each containing 2.22mg of Resazurin (redox indicator) and constantly flushed with nitrogen gas while adding the solution that contained dissolved and suspended calcium carbonate. Approximately 15g of ascorbic acid was added into these jars to provide enough ascorbate to maintain fully anaerobic conditions for long experiment duration. The reaction between calcium carbonate and ascorbic acid produces carbon dioxide gas

(Chem. Eq. 7), which further helps in driving off any dissolved oxygen. The jars were then tightly sealed using rubber electrical tape and allowed to cool down to room temperature so that they could be used for the sediment incubations. The pH of the calcium ascorbate solution was 7, a value that remained constant over the entire incubation period.

2.6 SEDIMENT INCUBATION

Since it was my goal to monitor production of new sulfate during the sediment incubation, it was of utmost importance that sulfate was not produced because of an artifact. For example, contamination of the sediment with oxidants, such as oxygen from air, would drive abiotic and biological sulfur oxidation to sulfate. To cope with this challenge, the following sediment incubation protocol was employed (Figure 3).

2.6.1 Incubation series 1

Inside a glove bag, I redistributed the collected sediments into six aluminum coated airtight bags marked 1, 2, 3, 4, 5 and 6 each fitted with Rhizon® samplers. Rhizon® samplers allowed sampling of pore-water at certain time intervals within the incubation period (Figure 4). I then placed a glass ampule, containing approximately 4ml of 0.037M ^{34}S-labeled sulfate solution and 1ml of ^{18}O-labeled water, into bags 1, 2, 3, 4 and 5. The sixth incubation bag was used as a control experiment. The ampule embedded in this bag contained 4ml of 0.037M ^{34}S-labeled sulfate, 1ml of ^{18}O-labeled water and 2ml of 1.25M sodium molybdate. Molybdate inhibits microbially mediated sulfate reduction (Carlson et al., 2015). Approximately 100ml of sulfate-free artificial seawater was added into each bag (Table 1). To ensure that this water was oxygen-free, nitrogen gas was bubbled through it before being added into the bags. Outside the glove bag each incubation bag was sealed on the edge of the open end one at a time using a 6-inch portable hand crimper heat sealer model

KF-150CS, while the other incubation bags were kept inside of the glove bag. During my initial bag sealing tests I used a 12-inch tabletop 8mm wide seal heat impulse hand sealer model IPK-308H manufactured by Impak Corporation. This sealer did not produce a tight seal on the aluminum-coated incubation bags whereas the model KF-150CS does. The sealing period – which means exposure to air – was kept as brief as possible to minimize contamination of the sediment by atmospheric oxygen. The sealed incubation bags were then transferred into three freezer bags filled with ascorbic acid solution. Each of these bags was in turn put into a glass pickle jar that was also filled with ascorbic acid, so that every pickle jar contained two incubation bags. These jars were then tightly sealed and kept at room temperature (Figure 4). These conditions do not reflect *in situ* conditions (9 ºC) but correspond to the conditions at which the sediments were stored, making it likely that the microbes adapted to the new conditions.

The purpose of the multiple container setup was to prevent oxygen from entering the incubation bags by employing three barriers, the first being the glass pickle jar containing ascorbic acid that acts as oxygen scrubber, the second being the freezer bag with ascorbic acid that again acts as oxygen scrubber, and finally the airtight incubation bag. Resazurin (redox indicator) dissolved in the ascorbic acid solution allowed me to observe if/when the outer glass jar compartment started to become oxidized (color change from clear to pink) and replace the solution before oxygen reached the inner freezer bag compartment.

While these precautions were expected to ensure that anaerobic conditions prevailed in and around of the sediment bag throughout the experiment duration, this was not the case for initial phase – i.e. the incubation of the sediment itself. Even the nitrogen environment in glove bag cannot guarantee that the sediment remains fully anaerobic during redistribution. For these reasons, there was a need to allow the sediments to fully regain their undisturbed state after sediment transfer.

This was achieved by allowing the experiment to stand for 2 weeks. After this resting period, I broke the glass ampules within the incubation bags, releasing $^{34}S_{SO4}$ and $^{18}O_{H2O}$ labels into the sediment. This was achieved by pressing the bag against a wooden block on a working bench taking caution not to cause any damage to the bag. Inside the glove bag under a nitrogen environment, I then conducted the first series of pore-water sampling. I periodically took pore-water samples that allowed me to monitor the concentration and sulfur isotope composition of sulfate and sulfide and the oxygen isotope composition of water and sulfate.

2.6.2 Incubation series 2

This set of incubation experiments started one week after completion of the first series. Two major adjustments were made in the experimental set up based on results obtained from the first set of experiments. 1) Artificial seawater modification - sediments were mixed with artificial seawater containing 5mM of sulfate. 2) Replacement of the inner ascorbic acid compartment with an anaerogen bag.

In the initial sediment preparation procedure, the sediments were mixed in a ratio of 50-50% with sulfate-free artificial seawater. Even in the first sampling time point, almost no sulfate could be recovered. We considered that there was little to no sulfate left in the sediment after the long storage, and that it might be possible that ascorbic acid penetrates into the incubation bag, acting as highly attractive substrate for sulfate reducing bacteria, causing rapid draw-down of sulfate concentrations. To address these issues, I added artificial seawater that contained 5mM of sulfate to constitute the sediment slurry. Also, the inner oxygen barrier bag was modified, by replacing the ascorbic acid with an anaerogen bag.

In detail, the collected sediments were redistributed into six aluminum coated airtight bags marked 1, 2, 3, 4, 5 and 6 each fitted with Rhizon® samplers. This was done inside a glove bag filled with

nitrogen gas to minimize contamination with atmospheric oxygen. I then placed a glass ampule, containing approximately 1ml of 0.037M ^{34}S-labeled sulfate solution and 1.5ml of ^{18}O-labeled water, into bags 1, 2, 3, 4 and 5. The sixth incubation bag was used as control experiment. The ampule embedded in this bag contained 1ml of 0.037M ^{34}S-labeled sulfate, 1.5ml of ^{18}O-labeled water and 2ml of 1.25M sodium molybdate which acts as sulfate reduction inhibitor. Unlike in the first experiment series, the solutions in the glass ampules were flushed with Argon gas prior to sealing in order to expel any dissolved oxygen. See section 2.4 for a detailed description of ampule production. Approximately 100ml of artificial seawater containing 5mM sulfate was added into each bag. To ensure that this solution was oxygen-free, nitrogen gas was bubbled through it before being added into the bags. The bags were heat-sealed one by one outside the glove bag using a 6-inch portable hand crimper heat sealer model KF-150CS. This period of exposure to air was kept as brief as possible to minimize contamination of the sediment by atmospheric oxygen. Three oxygen barriers – two compartments of ascorbic acid and airtight incubation bag were employed in the first series of experiments. The second series of experiments involved two oxygen barriers – one compartment of ascorbic acid and an airtight aluminum coated incubation bag. The outmost compartment consisted of three pickle jars filled with ascorbic acid solution. Each pickle jar contained two incubation bags placed in one freezer bag. While the freezer bags in the first series of experiments contained ascorbic acid, in the second series of experiments this ascorbic acid compartment was replaced by the use of an anerogen bag placed along with the incubation bags in the freezer bag. On contact with oxygen these bags emit heat spontaneously, an indication that they are still active. This confirms that no oxygen penetrated into the incubation bag in addition to monitoring color change from Resazurin. It is also important to note that these bags do not produce hydrogen gas, which could be used as a substrate by the sulfate reducers. The freezer bags were

then placed into the pickle jars containing ascorbic acid solution, tightly sealed and incubated at room temperature. The second adjustment involved modification of the oxygen barriers.

2.7 PORE-WATER SAMPLING

Pore-water sampling was done at different time intervals based on the modeling results. For both series of incubation experiments the first pore-water samples were taken after 2 weeks' resting period, immediately after releasing the isotope labels into the sediment. This resting period was necessary to allow the sediments to fully regain their undisturbed state after sediment transfer. Second and third (final) pore-water sampling during the first series of experiments were conducted after 53 and 81 days respectively, whereas during the second series of experiments samples were taken after every 10 days. The first aliquot (1 to 2ml) of the sampled water from every bag at every sampling time-point was presumed to be potentially contaminated, as it comprises the water that is located in the Rhizon® tube. This aliquot is prone to contamination with material from the Rhizon® sampler, and may contain oxidized sulfur. Consequently, the first aliquot was preserved for analysis of oxygen isotopes of water, which would not be affected by sulfur oxidation. Using six syringes each containing 1ml of 20% zinc acetate solution I drew pore-water from the bags (see table on results for volumes of pore-water extracted at every time-point). The zinc immediately reacts with sulfide preventing its oxidation to sulfate. The samples were then immediately processed to avoid contamination with oxygen from air, and to exclude potential oxidation of the zinc sulfide.

2.8 CHEMICAL ANALYSES

2.8.1 Concentration of sulfate and sulfide

Sulfide from pore-water was precipitated using zinc acetate. The zinc sulfide suspensions were

transferred from the syringes into six 15ml centrifuge tubes and centrifuged at 3500 rpm for 5 minutes. The supernatants were then filtered through 0.45µm membrane syringe filters into another set of clean 15ml centrifuge tubes, leaving behind zinc sulfide precipitates in the original centrifuge tubes. Concentrated hydrochloric acid (250µl) was added into each of the supernatants, shaken, while bubbling nitrogen gas through the solution for approximately 5 minutes. This ensured that any sulfide present was degassed as hydrogen sulfide. This also helped counter the buffer action of the acetate from the zinc acetate addition to lower the pH of the solution to 2. Pore-water sulfate was precipitated as barium sulfate by adding 1ml of 1M barium chloride solution. The white suspensions were then centrifuged at 3500 rpm for 5 minutes and the supernatants carefully removed using a 1ml pipette. The residues (precipitates) were washed twice with deionized water to remove dissolved ions such as excess barium and chloride ions. Using 5.5ml of 0.05M DTPA in 1M NaOH, I re-dissolved barium sulfate precipitates from the experiments. Diethylenetriaminepentaacetic acid (DTPA) is a strong complexing agent (chelator) for barium. I subsequently re-precipitated barium sulfate by the addition of 500µl of 12M HCl and 1ml of ~1M acidified barium chloride solution (Bao, 2006). This procedure helps liberate ^{18}O-spiked water trapped in the barium sulfate precipitate, and effectively removes this potential artifact. I washed barium sulfate precipitates with deionized water and acetone and allowed them to dry. Zinc sulfide precipitates were washed with deionized water and converted to silver sulfide. This involved addition of 2ml of 5% w/w silver nitrate solution followed by agitation and vortexing. The contents were allowed to sit in a dark place overnight to make sure the reaction was complete, and that no photo-oxidation of silver nitrate took place. The following day the samples were vortexed to break up any plugs and homogenize the sample. I then centrifuged the samples and decanted the supernatant. The precipitates were washed with 2ml of 1M ammonium hydroxide solution to

dissolve colloidal silver and any silver chloride solids, centrifuged, washed with deionized water and acetone and allowed to dry. Dried samples of barium sulfate and silver sulfide were used to determine the concentrations of sulfate and sulfide respectively. This was done in-house using gravimetric methods.

2.8.2 Sulfur and oxygen isotope analysis of sulfate, sulfide and water

For sulfur isotope analysis, approximately 0.45mg of barium sulfate and 0.50mg of silver sulfide was weighed into tin capsules. Respectively equal amounts of vanadium pentoxide, a catalyst that helps in the conversion of sulfate and sulfide to sulfur dioxide gas, were added into the capsules. The top of the capsule was then closed using tweezers and shaken vigorously to mix the catalyst with the sample. The capsules were then folded into a ball and combusted in an elemental analyzer (Elementar Pyrocube), and the produced sulfur dioxide gas was analyzed for sulfur isotope composition using a continuous-flow isotope ratio mass spectrometer (IsoPrime GeoVisION). Sulfur isotope values were reported relative to Vienna Canyon Diablo Troilite (VCDT). For oxygen isotope analysis of sulfate, about 0.45mg of barium sulfate together with graphite (0.4mg) and silver chloride (0.2mg) were weighed into silver capsules, carefully folded and pyrolized (absence of oxygen) in the elemental analyzer in presence of carbon to form carbon monoxide, which was then analyzed for isotope composition and isotope values reported relative to Vienna Standard Mean Ocean Water (VSMOW). For calibration of sulfur and oxygen isotopes values of sulfate, I used international standards, NBS-127, IAEA SO-5 and IAEA SO-6 as well as in-house standards and international standards S1, S2 and S3 for sulfur isotope values of sulfide. A different technique was used to pack water for oxygen isotope analysis. A firm-walled silver capsule was placed on capsule sealing press while adding 0.6 to 4.5mg of water sample with a micropipette. The capsule was then sealed instantly and pyrolized in an elemental analyzer as described above,

however, the produced CO gas was diluted to 8% of the original sample size in order to stay within the measurement capacities of the IRMS (i.e. avoiding of off-scale measurements). For comparison, deionized water was used, however, no calibration to international standards was performed, as the error on the highly labeled ^{18}O-water is approximately 30‰.

2.9 MODELING

For the design of my project I devised a numerical model that predicts the concentration and isotope trends of sulfate, sulfide and water over time for laboratory experiments in which sulfur and oxygen isotope labels are introduced into marine sediments where microbial sulfate reduction and sulfide oxidation co-occur. The model predictions can be used to determine the amounts of $^{34}S_{SO4}$ and $^{18}O_{H2O}$ label that are needed to be able to make quantitative observations about simultaneous oxidative-reductive sulfur cycling that, in absence of a label, would take years to be detectable, or would not be detectable at all.

2.9.1 Model development

In the studied incubations, the experimentally accessible variables are the concentration and isotope composition of residual sulfate and sulfide, as well as the oxygen isotope composition and pH of the pore-water. With the help of these variables it is possible to determine key parameters such as sulfate reduction rates, sulfur isotope fractionation, oxygen isotope exchange between sulfate and ambient water and oxygen isotope equilibrium value between sulfate and water. There are two basic sets of mass balance equations of equations that can be derived for determination of these parameters, one set for the concentration of the compounds of interest, and a second for their isotope composition. A description of the interlinked reactions is presented in Figure 5. Below, I develop the mass balance equations that correspond to these reactions. Table 2 provides a detailed

description of the abbreviations, and Table 3 lists the values that were used to calculate concentration and isotope trends.

Sulfate mass balance

The concentration of sulfate is influenced by the net sulfate reduction (FSR_{net}), which removes sulfate and by the addition of sulfate from sulfide oxidation (F_{ox}). This relationship can be described as the relationship between the derivative of the sulfate concentration after the time, and the removal and addition of sulfate, according to

$$\frac{\mathrm{d}}{\mathrm{dt}}\mathrm{SO}_4^{2-}(\mathrm{t}) = -FSR_{net} + F_{ox}\ . \qquad \text{Mod. Eq. 1}$$

Sulfur isotope mass balance for sulfate

The mass balance for sulfur isotope composition of sulfate considers that because of isotope fractionation during microbial sulfate reduction ($\varepsilon^{34}\mathrm{S}_{\text{sulfate-sulfide}}$), the removed sulfate is isotopically lighter than the sulfate ($\delta^{34}\mathrm{S}_{\text{sulfate}}(\mathrm{t})$) that stays back, and takes into account that sulfate derived from sulfide oxidation has the isotope signature of the oxidized sulfide ($\delta^{34}\mathrm{S}_{\text{sulfide}}(\mathrm{t})$). Consequently, the derivative after the time for the product between the sulfate concentration and the isotope composition of sulfate, is related to the impact of sulfate removal and addition as follows:

$$\frac{\mathrm{d}}{\mathrm{dt}}\left(\delta^{34}\mathrm{S}_{\text{sulfate}}(\mathrm{t}) \cdot \mathrm{SO}_4^{2-}(\mathrm{t})\right) =$$

$$-FSR_{net}(\delta^{34}\mathrm{S}_{\text{sulfate}}(\mathrm{t}) + \varepsilon^{34}\mathrm{S}_{\text{sulfate-sul}}\quad) + F_{ox} \cdot \delta^{34}\mathrm{S}_{\text{sulfide}}(\mathrm{t})\ . \qquad \text{Mod. Eq. 2}$$

Oxygen isotope mass balance of sulfate

The mass balance equations for the oxygen isotope composition of the sulfate is slightly more intricate than the sulfur isotope mass balance, because microbial sulfate reduction cannot be considered any longer as a net flux that removes sulfate. Sulfate-reducing microbes not only take up sulfate, they also return a considerable amount of sulfate back to the environment. Some of this

returned sulfate has a different isotope composition than the sulfate that was taken up, which is the cause for sulfur and oxygen isotope fractionation by these organisms (e.g. Brunner and Bernasconi, 2005). In the case of sulfur isotope fractionation, this process can be mathematically treated as a simple removal of sulfate with an associated isotope fractionation. This is no longer possible in the case of oxygen isotope fractionation, because the some of the oxygen in the returned sulfate originates from water, via oxygen isotope exchange between intermediate sulfur compounds with ambient water (Mizutani and Rafter, 1969; Fritz et al., 1989). Based on this reasoning, the derivative after the time for the product of the oxygen isotope composition of sulfate with the sulfate concentration depends i) on the isotope effect related to the total uptake of sulfate into the microbes, which is equal to the net sulfate reduction plus the flux of sulfate that is returned by the sulfate-reducing microbes ($FSR_{net} + const_{rev}$), ii) on the isotope signature of sulfate that is returned by the sulfate-reducing microbes ($const_{rev} \cdot (\delta^{18}O_{water} + \varepsilon^{18}O_{water\text{-}sulfate})$), and iii) on the oxygen isotope composition of sulfate that was derived from sulfide oxidation ($F_{ox} \cdot \delta^{18}O_{water}$):

$$\frac{d}{dt}\left(\delta^{18}O_{sulfate}(t) \cdot SO_4^{2-}(t)\right) =$$

$$-\left(const_{rev} + FSR_{net}\right) \cdot \delta^{18}O_{sulfate}(t) + const_{rev} \cdot \delta^{18}O_{rev} + F_{ox} \cdot \delta^{18}O_{water}(t)\,. \quad \text{Mod. Eq. 3}$$

Sulfide mass balance

The mass balance describing change in external sulfide concentration considers the addition of sulfide through sulfate reduction and sulfide loss through the oxidative pathway, which is essentially the opposite to Mod. Eq. 1:

$$\frac{d}{dt}H_2S(t) = -F_{ox} + FSR_{net}\,. \quad \text{Mod. Eq. 4}$$

Sulfur isotope mass balance of sulfide

In analogy to the sulfide mass balance, the change in the product of the sulfur isotope composition of sulfide with the sulfide concentration is the opposite of the change in the product of the sulfur

isotope composition of sulfate with the sulfate concentration (Mod. Eq. 2):

$$\frac{\mathrm{d}}{\mathrm{dt}}\left(\delta^{34}\mathrm{S}_{\mathrm{sulfide}}(\mathrm{t})\ \cdot \mathrm{H}_2\mathrm{S}(\mathrm{t})\right) =$$

$$-\delta^{34}\mathrm{S}_{\mathrm{sulfide}}(\mathrm{t}) \cdot F_{ox} + (\delta^{34}\mathrm{S}_{\mathrm{sulfate}}(\mathrm{t}) + \varepsilon^{34}\mathrm{S}_{\mathrm{sulfate-sulfi}}\ ) \cdot FSR_{net}\ . \qquad \text{Mod. Eq. 5}$$

Oxygen isotope composition of water

In the case of water, its oxygen isotope composition is influenced by overall rate of sulfate reduction and sulfide oxidation, and reversibility of the process, according to:

$$\frac{\mathrm{d}}{\mathrm{dt}}\left(\delta^{18}\mathrm{O}_{\mathrm{water}}(\mathrm{t}) \cdot\ \mathrm{H}_2\mathrm{O}(\mathrm{t})\right) =$$

$$(const_{rev} + FSR_{net}) \cdot \delta^{18}\mathrm{O}_{\mathrm{sulfate}}(\mathrm{t}) - (const_{rev} \cdot (\delta^{18}\mathrm{O}_{\mathrm{water}}(\mathrm{t}) + \varepsilon^{18}\mathrm{O}_{\mathrm{water-sulfate}})$$

$$+ F_{ox} \cdot \delta^{18}\mathrm{O}_{\mathrm{water}}(\mathrm{t}))\ . \qquad \text{Mod. Eq. 6}$$

2.9.2 Conversion of mass balance equations into equations that can be executed in a numerical model

In order to calculate isotope trends in a numerical model, it is necessary to convert the mass balance equations into equations that can be evaluated in discrete (incremental) time steps. To achieve this, I defined

$$\mathrm{t}_{\mathrm{inc}} = \Delta\mathrm{t} = \mathrm{t}_{\mathrm{i+1}} - \mathrm{t}_{\mathrm{i}}\ , \qquad \text{Mod. Eq. 7}$$

where i = 0, 1, 2…days.

Using this approach, the concentration of sulfate can be calculated as follows:

$$\mathrm{SO}_4^{2-}(\mathrm{t}_{\mathrm{i+1}}) = \mathrm{SO}_4^{2-}(\mathrm{t}_{\mathrm{i}}) - FSR_{net} \cdot \mathrm{t}_{\mathrm{inc}} + F_{ox} \cdot \mathrm{t}_{\mathrm{inc}}\ , \qquad \text{Mod. Eq. 8}$$

and the concentration of sulfide as:

$$\mathrm{H}_2\mathrm{S}(\mathrm{t}_{\mathrm{i+1}}) = \mathrm{H}_2\mathrm{S}(\mathrm{t}_{\mathrm{i}}) - F_{ox} \cdot \mathrm{t}_{\mathrm{inc}} + FSR_{net} \cdot \mathrm{t}_{\mathrm{inc}}\ . \qquad \text{Mod. Eq. 9}$$

To obtain a stepwise calculation of the sulfur isotope composition of sulfate, Mod Eq. 2 is re-written as:

$$\delta^{34}S_{sulfate}(t_{i+1}) \cdot SO_4^{2-}(t_{i+1}) =$$

$$\delta^{34}S_{sulfate}(t_i) \cdot SO_4^{2-}(t_i) - (\delta^{34}S_{sulfate}(t_i) + \varepsilon^{34}S_{sulfate-sulfid}) \cdot FSR_{net} \cdot t_{inc}$$

$$+ \delta^{34}S_{sulfide}(t_i) \cdot F_{ox} \cdot t_{inc}, \quad \text{Mod. Eq. 10}$$

whereas the sulfur isotope composition of external sulfide (Mod. Eq. 5) is calculated as:

$$\delta^{34}S_{sulfide}(t_{i+1}) \cdot H_2S(t_{i+1}) =$$

$$\delta^{34}S_{sulfide}(t_i) \cdot H_2S(t_i) - \delta^{34}S_{sulfide}(t_i) \cdot F_{ox} \cdot t_{inc} + (\delta^{34}S_{sulfate}(t_i)$$

$$+ \varepsilon^{34}S_{sulfate-sulfide}) \cdot FSR_{net} \cdot t_{inc}. \quad \text{Mod. Eq. 11}$$

Finally, the oxygen isotope composition of water (Eq. 6) is re-cast as,

$$\delta^{18}O_{water}(t_{i+1}) \cdot H_2O(t_{i+1}) =$$

$$\delta^{18}O_{water}(t_i) \cdot H_2O(t_i) + (const_{rev} + FSR_{net}) \cdot t_{inc} \cdot \delta^{18}O_{sulfate}(t_i)$$

$$- (const_{rev} \cdot t_{inc} \cdot (\delta^{18}O_{water}(t_i) + \varepsilon^{18}O_{water-sulfat}) + F_{ox} \cdot t_{inc} \cdot \delta^{18}O_{water}(t_i)), \quad \text{Mod. Eq. 12}$$

and the oxygen isotope composition of sulfate as:

$$\delta^{18}O_{sulfate}(t_{i+1}) \cdot SO_4^{2-}(t_{i+1}) =$$

$$\delta^{18}O_{sulfate}(t_i) \cdot SO_4^{2-}(t_i) - (const_{rev} + FSR_{net}) \cdot t_{inc} \cdot \delta^{18}O_{sulfate}(t_i) + (const_{rev} \cdot t_{inc} \cdot$$

$$(\delta^{18}O_{water}(t_i) + \varepsilon^{18}O_{water-sulfate}) + F_{ox} \cdot t_{inc} \cdot \delta^{18}O_{water}(t_i)) \quad \text{Mod. Eq. 13}$$

2.9.3 Model parameters

Sulfur and oxygen isotope fractionations caused by sulfate reduction have been linked to a sequence of enzyme-catalyzed isotope fractionation steps involving several intermediate sulfur compounds and a series of forward and backward fluxes (Rees, 1973; Habicht and Canfield, 1997; Brunner et al., 2005; Brunner and Bernasconi, 2005; Brunner et al., 2012; Wing and Halevy, 2014). To calculate $\delta^{34}S$ and $\delta^{18}O$ changes in sulfate, sulfide and water, the developed model uses a presumably representative sulfate reduction rate from the Aarhus Bay (0.00005pmols/l/day; Figure 6; Holmkvist et al., 2011) in combination with a set of other initial conditions, such as amount of label and artificial seawater added. In the model this rate is expressed as net flux for sulfate reduction (FSR_{net}). Microbial sulfate reduction is usually accompanied by hidden reverse oxidative processes within the metabolic pathway of sulfate reduction, which releases new sulfate into the external sulfate pool. Based on culture experiments, a maximum value of 2 for the ratio between reversible release of new sulfate and net sulfate reduction (theta_reverse) was predicted (Brunner et al., 2012). In the model, this value represents the ratio between constant for the reverse flow of sulfate ($const_{rev}$) and sulfate reduction rate (FSR_{net}), i.e. $const_{rev}$ = theta_reverse · FSR_{net}.

Similarly, theta_oxidation is calculated as a ratio between flux for sulfide oxidation (F_{ox}) and sulfate reduction rate (FSR_{net}; F_{ox} = theta_oxidation · FSR_{net}). As there is no knowledge of the actual size of this flux – i.e. the 'true cryptic sulfur cycle', an arbitrary value had to be chosen for the model. I picked a value of 0.01, based the reason that any cryptic sulfide oxidation must be small relative to the net sulfate reduction (e.g. 1%) because larger fluxes would not have gone undetected in the comparison between ^{35}S-tracer based and sulfate concentration based sulfate reduction rate studies (i.e. the discrepancy between the outcomes of those studies would have been exceedingly large). Simultaneously, if this hidden oxidative process was much smaller that the

picked value of 0.01, one would have to conclude that this process may not be of any importance at all.

The $\delta^{18}O$ of sulfate in natural environments is strongly influenced by sulfate reduction, disproportionation and re-oxidation of reduced sulfur compounds (Böttcher and Thamdrup, 2001; Böttcher et al., 2001; Aharon and Fu, 2003). Changes in $\delta^{18}O_{sulfate}$ of up to +17‰ (starting from a seawater sulfate value around 9.6‰) have been observed in interstitial waters of marine sediments (Böttcher et al., 1998; Böttcher et al., 1999; Ku et al., 1999; Aharon and Fu, 2000; Aharon and Fu, 2003). Fritz et al., 1989 observed oxygen isotope exchange between sulfate and water during bacterial sulfate reduction and reported fractionation values of 25‰, 27‰ and 29‰ at 30, 17 and 5 ºC, respectively. In a study based on quantum-chemistry of sulfate-water a new value for oxygen isotope fractionation was suggested between dissolved sulfate and water of 23‰ at 25 ºC (Zeebe, 2010). My model uses oxygen isotope enrichment value between water and sulfate ($\varepsilon^{18}O_{water\text{-}sulfate}$) of 27‰, which is in proximity of the empirically determined values from Fritz et al. (1989). For sulfide oxidation I directly picked the value for oxygen isotope composition of water ($\delta^{18}O_{water}$) excluding any isotope fractionation factor, because oxygen isotope fractionations during oxidative sulfur cycle typically scatter around 0‰. Overall, it has to be noted that the arbitrary choice of the values for the enrichment factors does not heavily impact the outcome of this study. Natural-abundance fractionations of oxygen and sulfur isotopes will be barely noticeable because heavily isotopically labeled compounds are introduced, rendering the subtle natural abundance isotope fractionations undetectable.

3. INSIGHTS AND RESULTS FROM MODELING

Using the developed numerical model, I planned the laboratory incubation experiments. The model enabled me to determine the appropriate sampling time interval, suitable sizes of the incubation bags, sediment pore-water ratio, pore-water sample volume and the amount of sulfate and water labels added into every incubation bag (Figure 7, 8).

a) It is easy to detect a change in the $\delta^{34}S$ of the sulfide when ^{34}S-labeled sulfate is used. My model clearly illustrates a noticeable change (more than 140‰) in sulfur isotope composition of the sulfide within a time period of 250 days (Figure 7b).

b) It is difficult to detect a change in the $\delta^{34}S$ of the sulfate when ^{34}S-labeled sulfate is used. My model results (Figure 7a) show that there is only a small change in $^{34}S_{SO4}$ in a time period of 250 days. To handle this setback, I tried to make my incubation experiments more sensitive by minimizing the amount sulfate concentration of the pore-water at the start of the experiment. This was achieved by using sulfate-free artificial seawater during my first series of incubation experiments. During the second series of incubations, sulfate concentrations in the sediment were adjusted by using artificial seawater that contained 5mM of sulfate.

c) To monitor the oxidative pathway from either intermediate sulfur compounds or sulfide back to sulfate, ^{18}O-labeled water can be used (simultaneous release of $^{34}S_{SO4}$ and $^{18}O_{H2O}$ into the sediment). Enrichment in ^{18}O of sulfate with increasing time during the experiment would suggest existence of a reverse (oxidative) process. My model predicted about 65‰ change in oxygen isotope composition of the sulfate within a period of 250 days (Figure 8).

This numerical model has some limitations. For example, isotope composition mass balances are only accurate when working with natural abundances of isotopes. Isotope labels were used in my experiments – for more accurate results isotopologue mass balances should be used instead.

4. RESULTS AND DISCUSSION

My project comprised four interlinked objectives, namely 1) the development of a protocol to produce isotopically labeled sulfate from isotopically labeled native sulfur and water, 2) the development of a sediment incubation method that minimizes/excludes contamination with atmospheric oxygen, 3) to experimentally determine the rates of sulfate reduction and oxygen incorporation from water into newly formed sulfate in a marine sediment, and 4) the development of a numerical model to predict the fate of sulfur and oxygen isotope labels that are introduced into an incubation experiment with marine mud (presented in modeling section).

4.1 A PROTOCOL FOR MAKING ISOTOPICALLY LABELED SULFATE

Several avenues for the production of isotopically labeled sulfate were explored. An attempt to oxidize native sulfur by using electrolytically produced bromine was unsuccessful because of exceedingly slow reaction kinetics. From this result it became apparent that sulfur oxidation with bromine would likely only be successful at elevated temperatures. Employing an autoclave, it is possible to reach temperatures above the melting point of sulfur, which is critical in increasing reaction rates. However, at such temperatures, bromine is extremely volatile and corrosive. Therefore, several serum bottle caps were tested: rubber stoppers, silicon stoppers with a Teflon (PTFE) membrane, and butyl stoppers with Teflon membrane. None of the stoppers could fully contain bromine, however, 20mm crimp-top aluminum seal with a gray septa made of butyl rubber that is covered with a film of Teflon was least degraded. A consequence of the leakage of bromine was that aluminum ions ended up in the experiment solution. Consequently, the method had to be refined such that the aluminum could be removed.

The final protocol for the production of isotopically labeled sulfate consists of the following nine steps:

- In the fume hood, weigh ^{34}S-native sulfur powder into a glass serum bottle; add deionized water and liquid bromine (Br_2).
- Cap the bottle using a 20mm crimp-top aluminum seal. This seal has protective gray septa made of butyl rubber coated with a film of Teflon (PTFE). Butyl rubber is resistant to oxidation by bromine.
- Place the serum bottle in 250ml beaker containing about 40ml of deionized water, and cover the top of the beaker with an aluminum foil. This serves as a trap for excess bromine from breaking out of the serum bottle to prevent damage/oxidation of the autoclave parts.
- Autoclave the beaker and its contents at 128 ^{o}C for 2 hours. This enhances the rate of the oxidation reaction. During this oxidation reaction bromine also reacts with aluminum seal as well as with the aluminum foil forming white solids of aluminum hydroxide at the neck of the serum bottle. This presents a risk of contamination to the sulfate solution by aluminum hydroxide.
- If this happens to be the case, these solids stuck at the neck of the bottle should be washed off using deionized water.
- The resulting solution is red-brown – due to excess liquid bromine. Boil this solution for about 10 minutes inside the fume hood to expel the excess bromine. Test the absence of bromine using pH indicator paper. Bromine bleaches the paper.
- Allow the solution to cool at room temperature and then filter through 0.45µm membrane syringe filter to remove any suspended solids.
- Neutralize the solution using sodium hydroxide. At pH of 7 white precipitates start to form in case there was contamination by aluminum hydroxide, i.e. aluminum hydroxide that was dissolved in the acid sulfate solution re-forms.

- These white precipitates should be filtered off using 0.45µm membrane syringe filters to obtain a clear ^{34}S-labeled sulfate solution.

4.2 A PROTOCOL FOR ANAEROBIC INCUBATION OF MARINE SEDIMENTS

- Before starting any experiment, test all the available equipment for its functionality.
- Distribute the collected sediments into aluminum coated airtight incubation bags fitted with Rhizon® samplers. Rhizon® samplers allow sampling of pore-water at certain predetermined time intervals during the incubation period. This procedure should be done inside a glove bag filled with nitrogen gas to minimize contamination with atmospheric oxygen.
- Place a glass ampule containing a mixture of ^{34}S-labeled sulfate solution and ^{18}O-labeled water, into the incubation bags. It is important to include a control experiment during incubations. In this control experiment the process of sulfate reduction is inhibited using 25mM sodium molybdate solution. The glass ampule for this control experiment contains ^{34}S-labeled sulfate solution and ^{18}O-labeled water and sodium molybdate.
- These solutions are flushed with argon gas before sealing the glass ampules.
- Add approximately 100ml of artificial seawater containing 5mM sulfate into each incubation bag. Nitrogen gas should be bubbled through this water to drive out any dissolved oxygen.
- Seal the bags each at a time outside the glove bag using a 6-inch portable hand crimper heat sealer model KF-150CS keeping the period of exposure to air brief as possible. This helps to minimize contamination of the sediment by atmospheric oxygen.
- Lay the incubation bags in freezer bags, place the freezer bags into glass pickle jars and cover the freezer bags with a solution of ascorbic acid. For full information on preparing

ascorbic acid solution refer to section 2.5. Ascorbic acid helps scavenge any atmospheric oxygen from outside. An anaerogen bag, which acts as an inner oxygen absorber is placed inside freezer bags along with the incubation bags. The jars are then tightly sealed and incubated at room temperature.

4.3 EXPERIMENTS

4.3.1 Series 1

No sulfate was recovered during the second sampling time point (T_1) from five incubation bags (1, 2, 3, 4 and 5; Table 4). This means that either there was little or no sulfate in the original storage bag or sulfate reduction was taking place at high rates (Figure 9). Some sulfate was precipitated from the control experiment (incubation bag 6), 1.7mM sulfate (T_1) and 0.69mM sulfate (T_2). This shows that molybdate at least to some degree inhibited the process of sulfate reduction.

It is possible that in the control experiment both barium molybdate (solubility product, 3.54×10^{-8} at 25 ^{o}C) and barium sulfate (solubility product, 1.08×10^{-10} at 25 ^{o}C) precipitate when barium chloride is added, since both compounds are insoluble in water. This would be problematic with respect to the oxygen isotope analysis of $BaSO_4$, particularly for experiments that are carried out with water enriched in ^{18}O. While sulfate does not exchange oxygen isotopes with water, molybdate readily exchanges its oxygen atoms with water. To counteract precipitation of barium carbonate, prior to adding barium chloride solution the pore-water was acidified using concentrated hydrochloric. Addition of acid in the control experiment led to a blue discoloration of the sample. This color change did not take place in the other experiments. I attribute the color change to the conversion of molybdate species (molybdenum IV) into molybdenum with the oxidation state V, which displays a blue color. The blue color was not visible in the precipitate,

but this does not rule out that barium molybdate may have co-precipitated. However, after the first precipitation of $BaSO_4$, the precipitate is re-dissolved to expel any ^{18}O-labeled water that is incorporated in small quantities into the barium sulfate crystals when the mineral is precipitated. During this step barium molybdate is dissolved. Upon re-precipitation, a major portion of molybdate is expected to remain in solution, as it is more soluble than barium sulfate. Finally, the sample obtained from the experiment with molybdate displayed the same sulfur yield (average of 85%) as the samples that did not contain any molybdenum. This indicates that the contribution of barium molybdate to the overall sample was negligible.

All sulfur isotope values for sulfate went off scale, as the ion beam for ^{34}S (corresponding to the mass 66 for $^{34}SO_2$) was too large. This is a result of the highly ^{34}S enriched sulfate label used in these experiments ($\delta^{34}S_{sulfate}$ > 200,000‰). The sulfur isotope composition of my sulfate samples averaged at 182,311‰, however, this value is meaningless in light of the fact that the full peak area of SO_2 with the mass 66 could not be captured. Data from the elemental analyzer of the Pyro Cube revealed that 85% of the sample analyzed was barium sulfate. Based on the detectable ion beam for ^{32}S (corresponding to the mass 64 for $^{32}SO_2$), it was estimated that approximately 7% of the barium sulfate was ^{32}S barium sulfate (Table 4). Of this barium sulfate, it is known that 1% of the detected ^{32}S was a contribution from the label (99% ^{34}S). The remaining 6% of the ^{32}S barium sulfate can then be attributed to the concentration of natural-abundance sulfate that was initially in this sediment. This allows for the calculation of the concentration of ^{32}S sulfate that was originally in this sediment to be approximately 37µmol/l. There was sharp increase in sulfur isotope values of sulfide between first time point (T_0), values ranged between 13-15‰ and second time point (T_1) values ranged between 2703-5990‰ (Figure 9b). This shows that sulfur was being transferred from the sulfate to sulfide pools through the process of sulfate reduction.

4.3.2 Series 2

This series of incubation experiments was planned after we learned that sulfate became depleted in the first series of incubations. In this second set of experiments we decided to adjust the sulfate concentrations of the artificial seawater added to the sediment. Unlike the first series of experiments where sulfate-free artificial seawater was used, during the second set of incubations the artificial seawater used contained 5mM of sulfate (Table 5).

Incubation bags 1, 3 and 5 showed a consistent decrease in sulfate concentration with time, (see Figure 10a). The sulfate concentration remained fairly constant (average of 1.8mM for the three sampling time points, with a slight decline of maximally 0.4mM) in the control experiment where molybdate was used to inhibit sulfate reduction (Figure 10b). Bag 1 had abnormally low sulfate concentrations at the first sampling time point. It is possible that more seawater was added to this bag relative to the amount of ^{34}S-sulfate label added compared to the other bags, an interpretation that is corroborated by the finding that the oxygen isotope composition of the water (dilution of added $^{18}O_{H2O}$ label) was also much lower (1877‰) than in the other incubation bags (Table 5). We also observed low sulfate concentrations in bag 6 during the first sampling time point. A competition between sulfate and molybdate ions for barium ions in the precipitation could be the cause of the observed low sulfate concentrations (non-quantitative sulfate precipitation). The precipitated barium molybdate is washed away in subsequent sample preparation steps, this compound does not contribute to the determined sample weight. Incubation bags 1, 3, 4 and 5 revealed a strong enrichment in $\delta^{18}O_{sulfate}$ (at least 800‰) within a time period of 33 days, whereas the $\delta^{18}O_{sulfate}$ of the control experiment remained fairly constant, approximately 13‰ (Figure 11). This is a clear indication that molybdate inhibited dissimilatory sulfate reduction.

5. INTERPRETATION

5.1 EXPERIMENT SERIES 1

Sulfate was likely immediately consumed in all the incubation bags other than the control experiment, as no sulfate could be retrieved at the second sampling time point (Figure 9). This is an indication that sulfate-reducing microbes were active from the initiation of the experiments. There are three possible explanations for the observed rapid sulfate depletion: (1) The bag that contains the original sediment is not fully airtight, leading to constant sulfate supply from sulfide oxidation, which was cut off once the sediments were transferred into the experiment bags. (2) It is possible that ascorbic acid (organic substrate for sulfate reducing organisms), which I used as oxygen scrubber, leaked into the incubation bags increasing the rates of sulfate reduction. (3) Finally, cryptic sulfur cycling indeed takes place in the investigated sediments.

It is likely that oxygen was breaking into the original sediment bag causing production of sulfate through oxidation of sulfide. When we opened the freezer box that contained the original sediment bags we could smell hydrogen sulfide gas. This was not only an indication that sulfate reducers were still active and alive, but also that it is likely that if sulfide escapes from the bags, oxygen can also penetrate into the bags. Therefore one can conclude that sulfide oxidation took place at all times, which supplied at least some sulfate for the survival of sulfate reducing microbes. Our estimates for initial sulfate concentrations, 37µmol/l fall within the range of postulated sulfate concentration values of 20-100µmol/l below the sulfate methane transition (Brunner et al., 2016). This is intriguing, because it might indicate that sulfate reducing organisms will not deplete sulfate to levels below of 30µmol/l, which might be connected to the energy limitations of microbial sulfate reduction, i.e. below this threshold, sulfate reduction may not be energetically feasible.

5.2 EXPERIMENT SERIES 2

In the first series of incubation experiments we noted that the original mud contained very low sulfate concentrations during our first sampling time point. These sulfate concentrations either dropped to immeasurable levels or the sediment became depleted of sulfate. Due to this observation, I decided to increase the initial sulfate concentration by the use of artificial seawater containing 5mM sulfate. Due to 50-50% ratio of sediment to artificial seawater the final concentration sulfate in each incubation bag was approximately 2.5mM. There was a rapid reduction in sulfate concentrations within 33 days, (Figure 10a, Table 5). Based on the decline in sulfate concentrations, one can calculate maximum sulfate reduction rates based on the difference between highest and lowest sulfate concentrations (Table 6). These rates of sulfate reduction are approximately three orders in magnitude higher than the published rates of 0.00005mmol/l/day (Figure 6, Holmkvist, Ferdelman, et al., 2011) for deep biosphere sulfate reduction used in my model. Even the control experiment had approximately 400 times higher sulfate reduction rates than the deep biosphere sulfate reduction rates. This shows that molybdate did not fully inhibit sulfate reduction, or that assimilatory sulfate uptake pathways may have played an important role. The extremely slow or non-existent oxygen isotope exchange between sulfate and water for the control experiment, corresponding to a ratio of 0.0055 between the oxygen exchange rate and sulfate removal rate, is intriguing, because it appears that some sulfate appears has been consumed (Figures 10b, 11b, 12). Notably, this exchange is on the same order of magnitude as the published deep biosphere sulfate reduction rates of 0.00005mmol/l/day. Either, inhibition with molybdate alters the sulfate reduction pathway in a manner where the process becomes less reversible, or dissimilatory sulfate reduction was fully inhibited, and the decline in sulfate concentrations would have to be attributed to assimilatory processes. If the latter is the case, the slow increase in the

oxygen isotope composition of sulfate could be considered to represent the elusive fingerprint of cryptic sulfur oxidation (Figure 11b).

The oxygen isotope data from the barium sulfate samples in the five bags (1, 2, 3, 4 and 5) show massive ^{18}O label transfer between water and sulfate. This can be attributed to the high rates of sulfate reduction, which as result brings about high oxygen exchange rates between water and sulfate. The obtained ratios between oxygen isotope exchange and net sulfate reduction are in a range between 0.2 and 0.45 (Figure 12a, based on Brunner et al. 2012). Such values are typical for many laboratory incubation experiments with sulfate reducers, but much lower than what has been observed for experiments carried out with mixed cultures from the environment, such as an exchange of 2.5 for sediments from Danish waters (Farquhar et al., 2008, Brunner et al. 2012). This finding, together with the observation of extremely rapid sulfate reduction rates underlines that our incubations operated fundamentally different from what is expected in the natural environment. Apparently, the extended sulfate-starvation of the sediment bags during storage led to the accumulation of organic substrates that are extremely favorable for sulfate reducing organisms, and once sulfate was supplied, these organisms rapidly responded to this opportunity.

6. Conclusions and Outlook

I developed experimental protocols that allow for the monitoring of cryptic sulfur cycling with the help of $^{34}S_{SO4}$ and $^{18}O_{H2O}$ labels that are released from ampules embedded in sediment incubations, which are kept strictly anaerobic. To do so, I established a method for making isotopically labeled sulfate by the use of an autoclave, a method can also be used to make a double-labeled sulfate (i.e. a combination of ^{34}S and ^{18}O-labels). An improvement of the method in the future would be to close the reaction vessels with glass stoppers, which would resolve the corrosion issues caused by bromine. The pickle-jar incubation method, combined with ascorbic acid as oxygen scavenger is an efficient approach for strictly anaerobic incubations. It is particularly appealing for applications in settings where technologically advanced equipment, such as an anaerobic chamber, is unavailable. This is often the case on sea-going research expeditions, which serve to collect the marine mud needed for research on cryptic sulfur cycling. The release of the labels and inhibitors from within the incubation bags with the help of ampules is an approach that alleviates the challenges encountered with introducing labels or inhibitors from outside, removing a potential source of contamination and disturbance.

The implemented numerical model can be used in the future by anyone who would like to carry out similar experiments, and will aid both in the planning of the experiments, as well as in the interpretation of the obtained results. However, in the future the model should be refined to directly calculate the concentrations of individual isotopes, and the molecules that contain these isotopes (isotopologues). Currently, the model uses δ-values, which can introduce errors when using strongly labeled materials.

The incubation experiments resulted in the surprising finding that once sulfate is introduced, sulfate reduction rates are extremely high. The rate of oxygen isotope exchange between sulfate

and water mediated by sulfate reducing microbes was similar to pure culture incubations. Apparently, during the long storage of the sediments, the sulfate-reducing microbes ran out of sulfate, and were limited to the supply from sulfate from oxidative processes, fueled by oxygen that diffused into the storage bags. These considerations lead to the conclusion that the lack of sulfate as terminal electron acceptor led to the accumulation of organic substrates that are favorable for sulfate reducing microbes. Once sulfate was supplied, sulfate reduction immediately proceeded at astonishingly high rates. Clearly, my incubation experiments cannot considered to be representative for cryptic sulfur cycling in marine sediments. Future experiments should use freshly retrieved marine sediments, or sample storage needs to be such that a steady supply with sulfate is ensured. The latter could be achieved by adding solid gypsum to the bags, which will slowly dissolve. If, for culturing, sulfate-restricted conditions for experimental work is needed, one could simply remove the remaining solids. However, such an approach would lead to an overprinting of the sulfur and oxygen isotope composition of dissolved sulfate with the isotope composition of the gypsum.

Despite the fact that my incubations are not representative for marine sediment, I was able to make key observations that can contribute to the body of research on cryptic sulfur cycling. The initial concentration of sulfate in the bags was approximately 37μM, a value that is similar to what has been postulated as sulfate concentrations below the sulfate methane transition. Apparently, even the high availability of organic substrates for the sulfate reducing microbes in the storage bags did not allow sulfate-reducing organisms to lower the sulfate concentration even further. This implies that there is a link between sulfate concentrations, and energetic threshold for dissimilatory sulfate reduction. A threshold value of 30μM for sulfate concentrations could be used for the study of the

thermodynamic limits of sulfate reduction, and to answer the question is there is a bioenergetic minimum quantum with respect to this process.

Last but not least, the inhibition of sulfate reduction with the help of molybdate revealed that sulfate consumption continues to proceed at low rates, however, with very little associated oxygen isotope exchange between sulfate and water. Potentially, inhibition with molybdate alters the sulfate reduction pathway in a manner where the process becomes less reversible. This possibility offers a new avenue to study the mechanisms of stepwise sulfate reduction by or dissimilatory sulfate bacteria. Alternatively, the decline in sulfate concentrations could be attributed to assimilatory processes. If this is the case, the slow increase in the oxygen isotope composition of sulfate would represent the elusive fingerprint of cryptic sulfur oxidation.

7. TABLES

Table 1. Chemicals selected for artificial seawater.

Solution	Chemical	Info	LOT #
SF-ASW	NaCl	Sodium Chloride ACS 99.0% Crystalline 2 kg Alfa-Aesar	P26B015
	$MgCl_2$	Magnesium Chloride Hexahydrate ACS 99.0%-102% Crystalline Alfa-Aesar	K07Z041
	$CaCl_2$	Calcium Chloride di-hydrate 99% min Granular 500 g Alfa-Aesar	M20A038
	KCl	Potassium Chloride 99% 1000 g Alfa-Aesar	10179997
	KBr	Potassium Bromide Ward's Science Cat#: 9421004	2012071675
	$NaHCO_3$	Sodium Hydogen Carboate Puratonic 99.998% 10 g	10184273
	H_3BO_3	Boric Acid 99+% 500 g	B10Y026
	$SrCl_2 \cdot 6H_2O$	Strontium Chloride Hexahydrate ACS 99.0%-103% Granular	T13B052

Table 2. Description of expressions and abbreviations.

SO_4^{2-}	concentration of external sulfate
H_2S	concentration of external sulfide
H_2O	amount of water
$\delta^{34}S_{sulfate}$	sulfur isotope composition of external sulfate
$\delta^{34}S_{sulfide}$	sulfur isotope composition of external sulfide
$\delta^{18}O_{sulfate}$	oxygen isotope composition of sulfate
$\delta^{18}O_{water}$	oxygen isotope composition of water
$\frac{d}{dt}$	differential operator
Δt	change in time
t_{inc}	time increment
FSR_{rev}	flux of reversible steps during sulfate reduction
F_{ox}	flux of sulfide oxidation to sulfate
FSR_{net}	net flux for sulfate reduction
$const_{rev}$	constant for reverse flow in sulfate reduction pathway
$\varepsilon^{34}S_{sulfate\text{-}sulfide}$	sulfur isotope enrichment for the reduction of sulfate to sulfide
$\varepsilon^{18}O_{water\text{-}sulfate}$	oxygen isotope enrichment between water and sulfate

Table 3. Applied parameters.

FSR_{net}	0.00005mmol/l/day (based on Aarhus Bay sediments)
F_{ox}	0.0000005mmol/l/day (arbitrary assumption, see text)
$const_{rev}$	product of Theta_reverse with FSR_{net}
$\varepsilon^{34}S_{sulfate\text{-}sulfide}$	-60‰ (upper range for sulfur isotope fractionations, because of expected refractory nature of organic matter)
$\varepsilon^{18}O_{water\text{-}sulfate}$	+27‰ (close to values observed by Fritz et al., 1989)
t_{inc}	0.5 days (chosen to run model within a reasonable number of cells in excel spreadsheet for a total planned experiment duration of 250 days)
Initial H_2O	100ml (estimate based on incubation bag size)
Initial SO_4^{2-}	14mmol/l (assumption based on location from where sediment was collected)
Initial H_2S	0.5mmol/l (based on location from where sediment was collected)
Initial $\delta^{18}O_{sulfate}$	+8.6‰ (reasonable value based on seawater sulfate value)
Initial $\delta^{18}O_{water}$	0‰ ($\delta^{18}O$ of seawater is close to 0‰)
Initial $\delta^{34}S_{sulfate}$	+21‰ (assumption based seawater sulfate value)
Initial $\delta^{34}S_{sulfide}$	-39‰ (assumption based on seawater sulfide value)
Theta_reverse	ratio between $const_{rev}$ and FSR_{net}, here 2 (Brunner et al., 2012)
Theta_oxidation	0.01 (arbitrary value, see text)
Pure $^{34}S_{sulfate}$ label	0.000117647mol/l (model chosen value, for preferable ^{34}S transfer during sulfate reduction)
98% $^{18}O_{water}$	1ml (model chosen value, produces a reasonable $\delta^{18}O$ change in sulfate within 250 days)
Isotope labels	released after 2 weeks (resting period to allow the sediment recover their undisturbed state after sediment transfer)

Table 4. Experiment Series 1.

Incubations	Name	Time point	Time (days)	Pore-water (ml)	$BaSO_4$ (mg)	Ag_2S (mg)	Sulfate (mmol)	Sulfate (mM)	Sulfide (mmol)	Sulfide (mM)	S Yield % EA	^{32}S Yield % IRMS	$\delta^{34}S$ (VCDT)	Comment
Bag 1	Ag_2S	T_0	0	4.4		2.60			0.0105	2.38	79	79	15.2	
	Ag_2S	T_1	53	2.3		0.78			0.0031	1.36	68	60	3370.1	
	$BaSO_4$	T_0	0	4.4	3.6		0.015	3.5			90	7	159843.0	offscale
Bag 2	Ag_2S	T_0	0	4.8		1.81			0.0073	1.52	82	81	14.6	
	Ag_2S	T_1	53	5.5		1.40			0.0056	1.03	72	59	5989.9	offscale
	$BaSO_4$	T_0	0	4.8	5.9		0.025	5.3			83	6	175754.8	offscale
Bag 3	Ag_2S	T_0	0	2.6		0.77			0.0031	1.19	93	76	13.4	
	Ag_2S	T_1	53	4.4		1.23			0.0050	1.13	78	67	4677.6	offscale
	$BaSO_4$	T_0	0	2.6	3.1		0.013	5.1			116	11	186118.0	offscale
Bag 4	Ag_2S	T_0	0	4.4		1.00			0.0040	0.92	75	76	12.9	
	Ag_2S	T_1	53	5.25		2.48			0.0100	1.91	78	70	2702.7	
Bag 5	Ag_2S	T_0	0	3.5		1.34			0.0054	1.55	75	75	14.1	
	Ag_2S	T_1	53	4		1.14			0.0046	1.15	75	68	3219.4	
Bag 6	Ag_2S	T_0	0	3		0.56			0.0022	0.75	71	69	13.1	
	Ag_2S	T_2	81	27		0.60			0.0024	0.09	6	6	13.7	
	$BaSO_4$	T_0	0	3	3.4		0.014	4.8			82	7	205857.9	offscale
	$BaSO_4$	T_1	53	4.1	1.6		0.007	1.7			86	7	183983.6	offscale

Table 5. Experiment Series 2.

Incubations	Time point	Time (days)	Pore-water (ml)	$BaSO_4$ (mg)	Sulfate (mmol)	Sulfate (mM)	O yield % IRMS	δ^{18}Osulfate IRMS (VSMOW)	δ^{18}Owater IRMS (VSMOW)
Bag 1	T_0	0	3.5	1.3	0.006	1.6	91.1	9.6	
	T_1	13	9	3.3	0.014	1.6	104.0	117.0	
	T_2	23	10	2.7	0.011	1.1	100.0	365.8	1877.2
	T_3	33	10	1.0	0.004	0.4	80.1	868.6	
Bag 2	T_0	0	3	1.7	0.007	2.4	99.8	14.2	
	T_1	13	8.4	5.1	0.022	2.6	87.4	188.9	
	T_2	23	9.5	3.0	0.013	1.4	100.5	764.7	3603.3
	T_3	33	10.2	0.3	0.001	0.1			
Bag 3	T_0	0	4	2.7	0.012	2.9	84.2	13.5	
	T_1	13	10	6.1	0.026	2.6	125.3	236.1	
	T_2	23	11	4.4	0.019	1.7	100.7	633.4	4062.3
	T_3	33	11	1.4	0.006	0.6	89.5	1490.2	
Bag 4	T_0	0	3.2	1.9	0.008	2.5	114.5	17.1	
	T_1	13	9.4	7.7	0.033	3.5	106.7	226.6	
	T_2	23	10	4.1	0.018	1.8	100.2	671.4	3935.7
	T_3	33	10.2	1.1	0.005	0.5	83.8	1543.8	
Bag 5	T_0	0	4	2.7	0.012	2.9	108.7	14.1	
	T_1	13	10.5	6.9	0.030	2.8	107.7	182.5	
	T_2	23	10.6	5.3	0.023	2.1	101.8	490.1	3828.6
	T_3	33	11.7	1.9	0.008	0.7	93.1	1267.3	
Bag 6	T_0	0	3.6	1.4	0.006	1.7	97.3	14.2	
	T_1	13	9.5	4.6	0.020	2.1	99.4	12.7	
	T_2	23	10	4.4	0.019	1.9	100.8	12.5	3579.6
	T_3	33	11	4.3	0.018	1.7	101.2	15.0	

Table 6. Experiment Series 2 Sulfate reduction rates.

Incubation bag	Conc. change (mmol/l)	Days	Rates (mmol/l/day)	Factor 1	Factor 2
1	1.2	20	0.06	1150	12
2	2.5	20	0.12	2483	25
3	2.1	20	0.10	2072	21
4	3.0	20	0.15	3029	30
5	2.1	20	0.11	2130	21
6	0.4	20	0.02	408	4

Factor 1 refers to a sulfate reduction rate typical for the deep biosphere, whereas factor 2 refers to sulfate reduction rates typical in the top 30 cm of sediment (Figure 6). Values for this comparison were taken from Holmkvist et al. (2011).

8. FIGURES

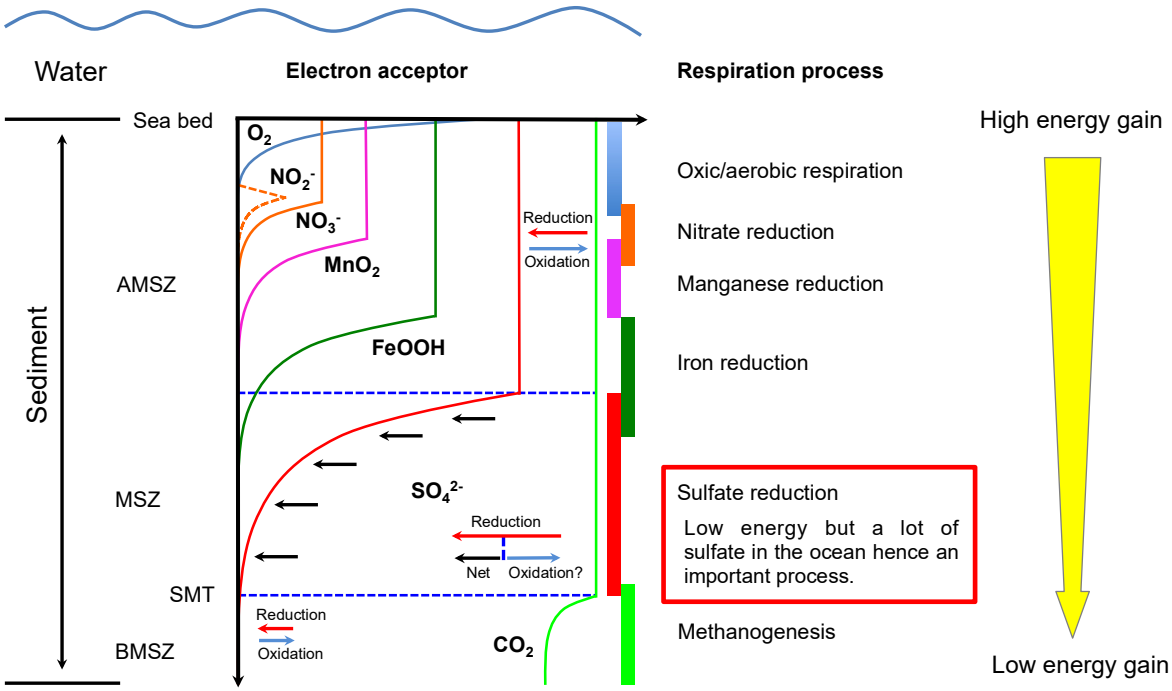

Figure 1. Geochemical zonation in marine sediments.
Depth distribution of common electron acceptors and the respective main microbial energy-deriving processes that drives various metabolic processes within these zones. SMT, MSZ, AMSZ and BMSZ represent the sulfate methane transition, main sulfate zone, above main sulfate zone and below main sulfate zone respectively. SMT is a chemical boundary that separates sulfate reduction and methanogenic zones. Redox arrows in AMSZ and BMSZ illustrate the potential existence of concomitant sulfur oxidation and reduction that compensate for each other, so that no net sulfate/sulfide production or consumption is observed in these two zones (modified after Canfield and Thamdrup, 2009).

Figure 2. A map showing Skagerrak and Kattegat where sediments were retrieved.

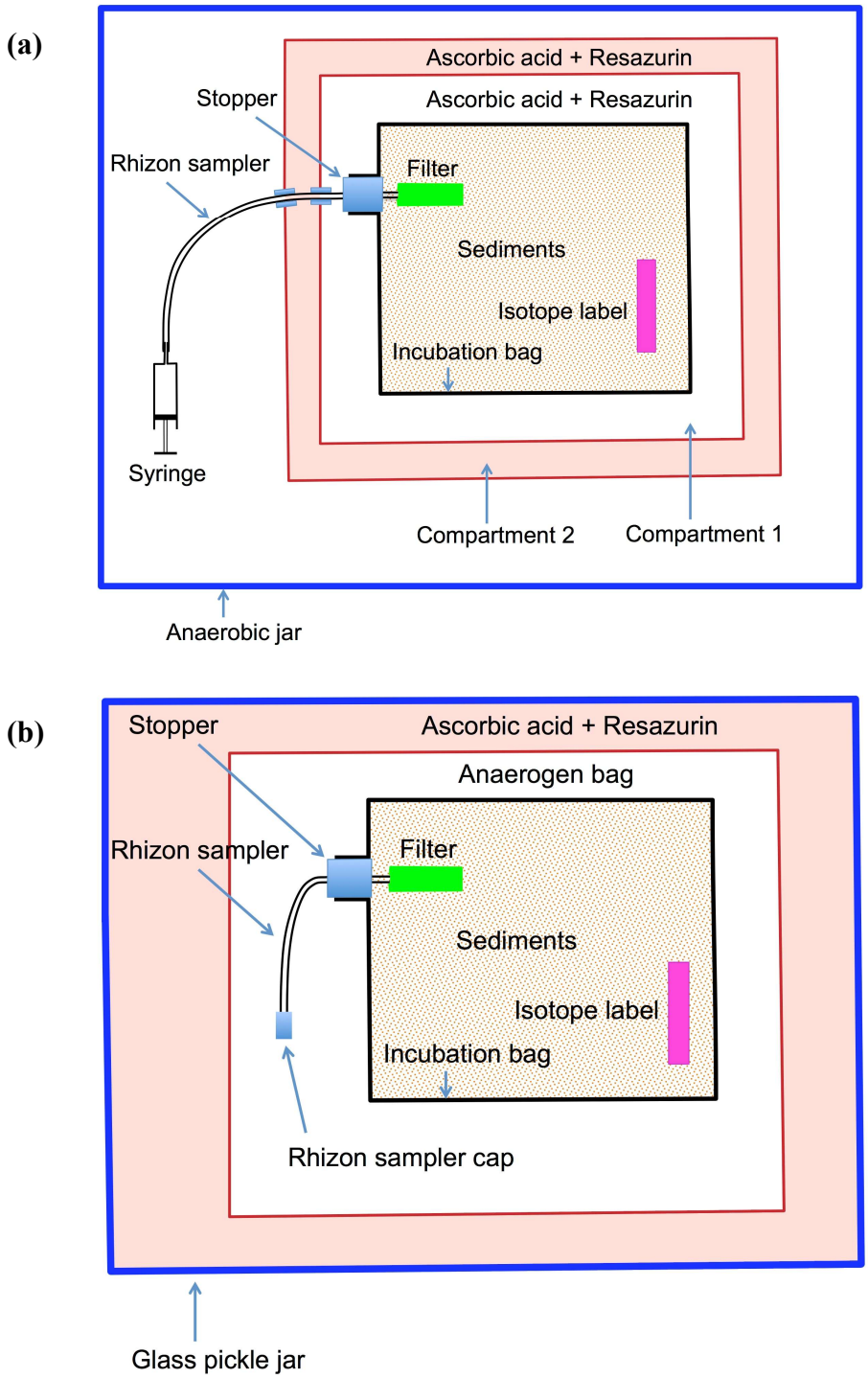

Figure 3. Sediment incubation set-up.
(a) A schematic representation of laboratory sediment incubation set-up employed in incubation series 1. (b) Set-up used in incubation series 2. Ascorbic acid acts as an oxygen scavenger to prevent the oxidation of the sediments by atmospheric oxygen. Rhizon® samplers are filter membranes that allow pore-water sampling by applying a vacuum via a disposable plastic syringe that is connected to the end of the sampler.

(a)

(b)

Figure 4. Sampling procedures.
(a) Pore-water sampling inside a glove bag. The bag was flushed several times with nitrogen gas (N_2) and then filled with N_2 to maintain oxygen-free conditions during sampling and (b) Laboratory sediment incubation experiments. The sediment is sealed in aluminum coated foil bags, which are placed in pickle jars. The jars are filled with water that contains ascorbic acid that acts as an oxygen scavenger to prevent oxidation of the sediments by atmospheric oxygen. Resazurin was added as a redox indicator, which is pink in presence of oxygen, and clear under anaerobic conditions.

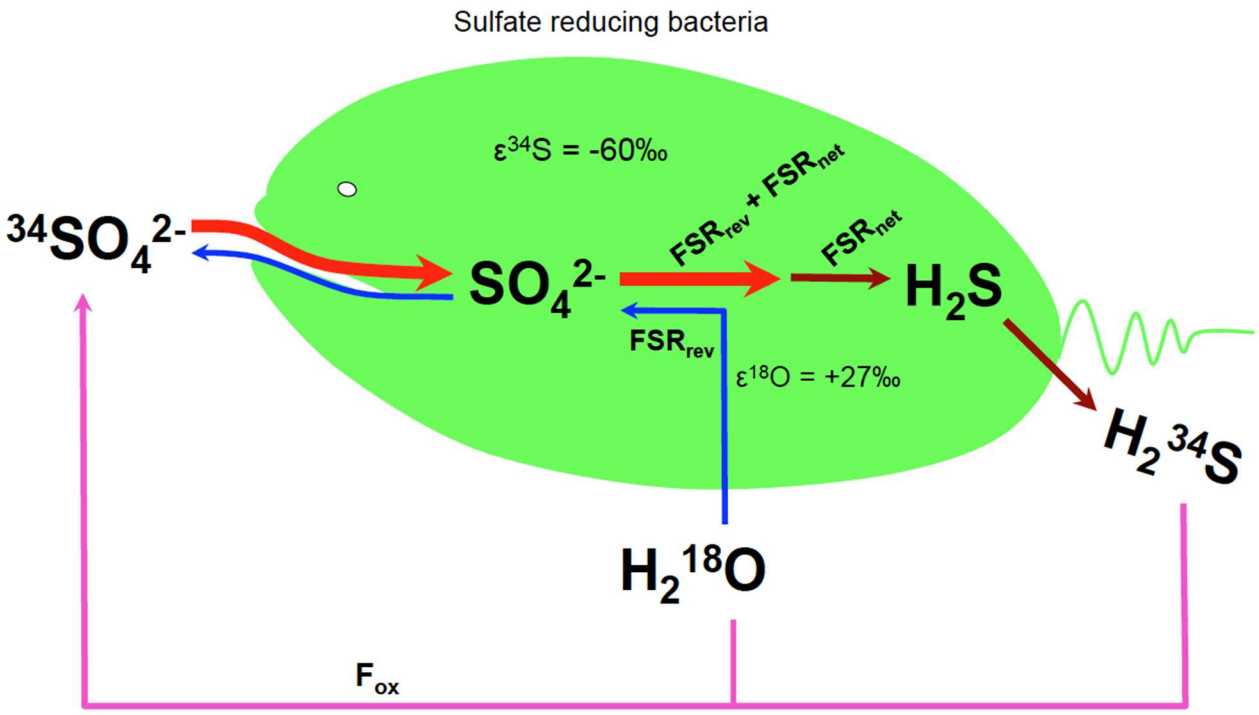

Figure 5. A simplified model for microbial sulfate reduction and oxidation processes.
Sulfur isotope composition of the sulfide that leaves the microbe is altered by kinetic sulfur isotope effects related to the stepwise reduction of sulfate to sulfide, while oxygen isotope composition of sulfate is modified by equilibrium isotope exchange effects between sulfur-oxy intermediates and water. For abbreviations, see Table 2.

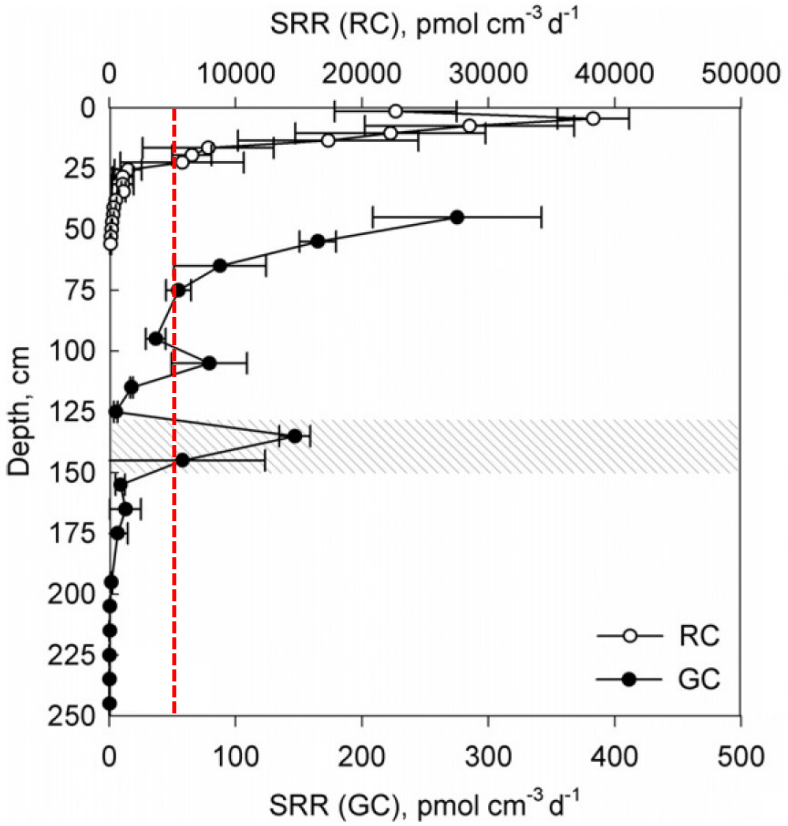

Figure 6. Sulfate reduction in shallow sediments and the deep biosphere.
The intersections of the dashed line with the sulfate reduction rate curve at 25cm and at 100cm were taken as comparison for the rates obtained in my bag experiments (Table 6) (Figure from Holmkvist et al. 2011).

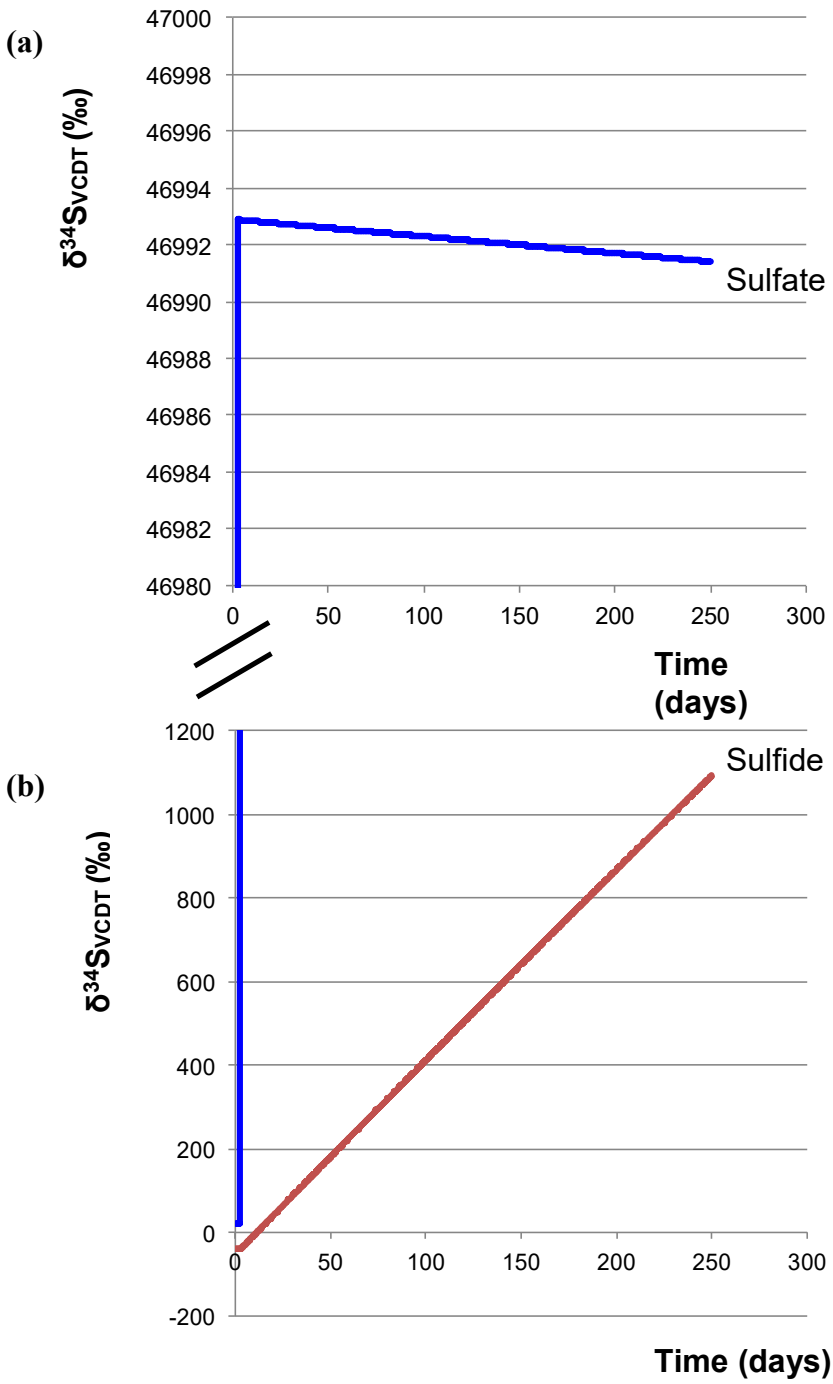

Figure 7. Predicted isotope trends for $\delta^{34}S$ of sulfate (Figure 7a) and sulfide (Figure 7b) after addition of the sulfate label.
Different scales have been used for the y-axis when plotting the graphs. This is because the change in $\delta^{34}S$ of the sulfate is so small compared to that of sulfide. A bigger y-axis scale in Figure 7a makes the change in $\delta^{34}S$ of the sulfate noticeable.

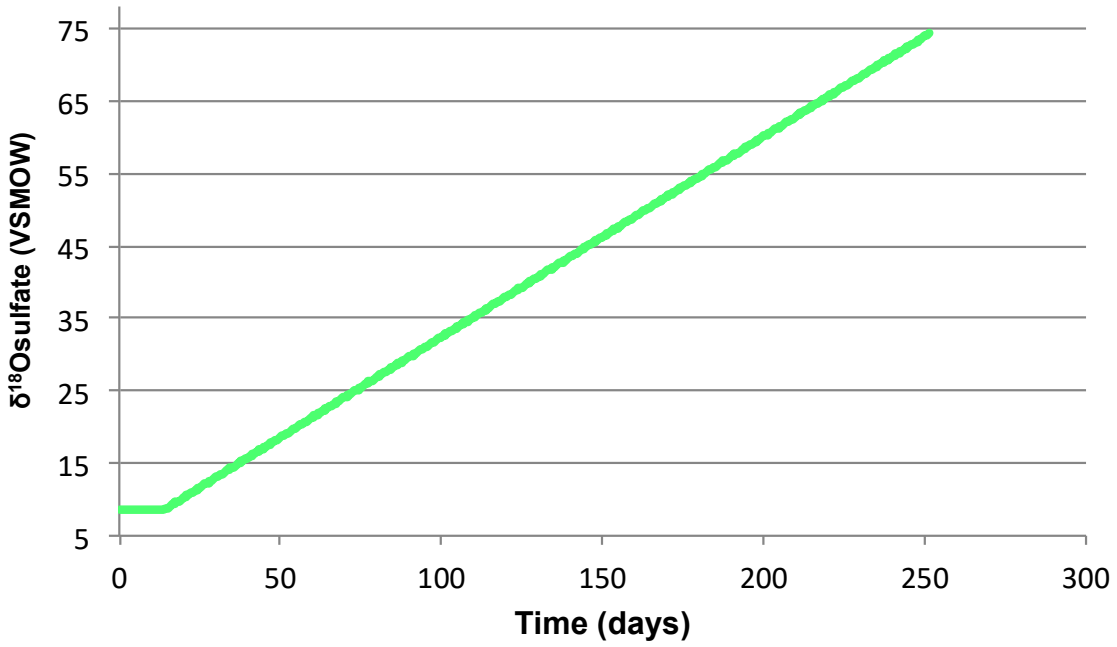

Figure 8. Predicted isotope trends for $\delta^{18}O$ of sulfate after addition of the ^{18}O-labeled water.

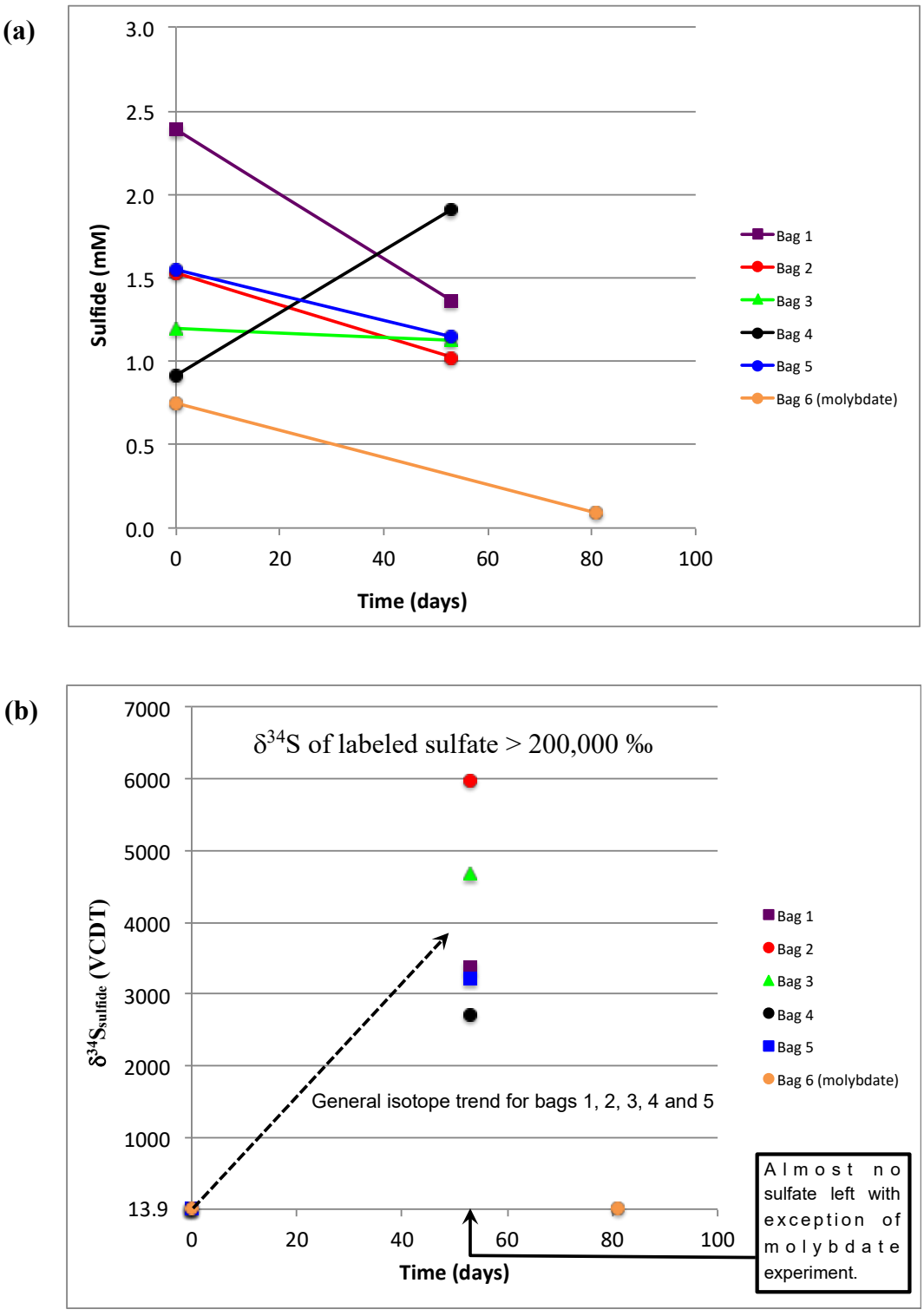

Figure 9. (a) Sulfate concentration trends in incubation series 1. (b) Sulfur isotope trends of sulfide in incubation series 1.

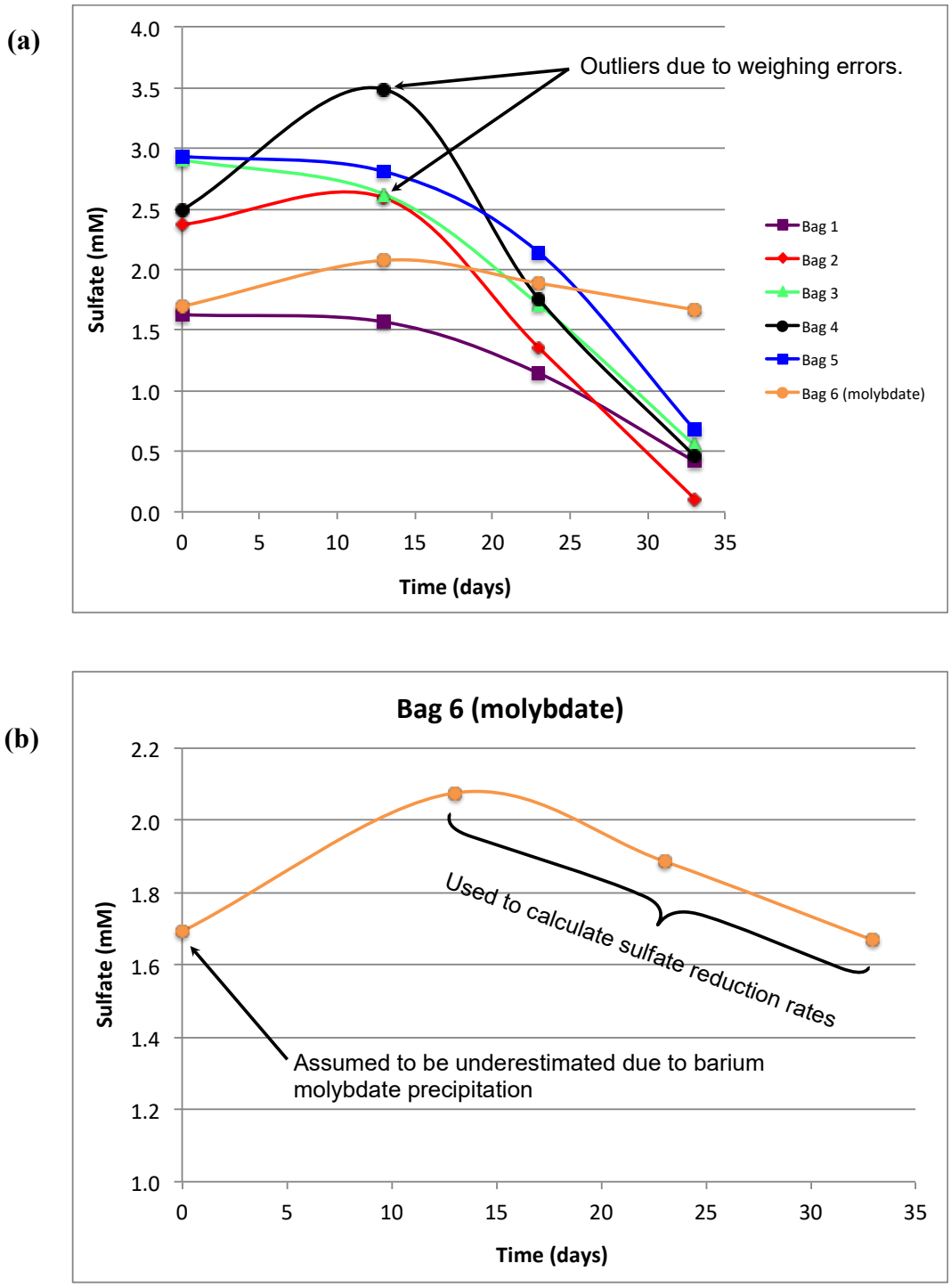

Figure 10. Results of incubation series 2.
(a) Sulfate concentration trends in incubation series 2. (b) Sulfate concentration trend in the molybdate experiment plotted on a different scale. Smooth curved lines display overall trends.

(a)

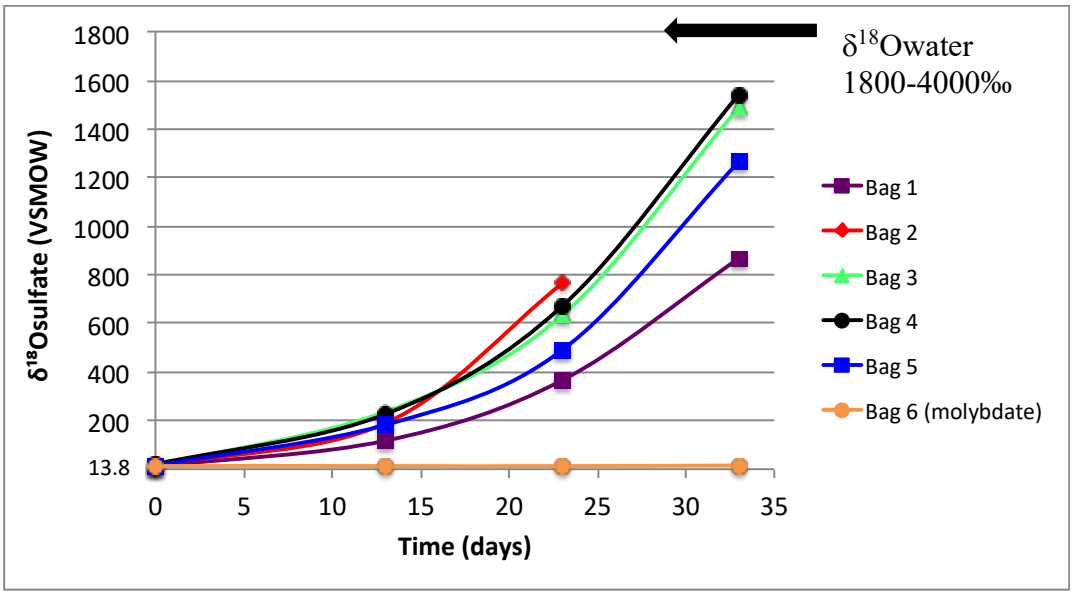

(b)

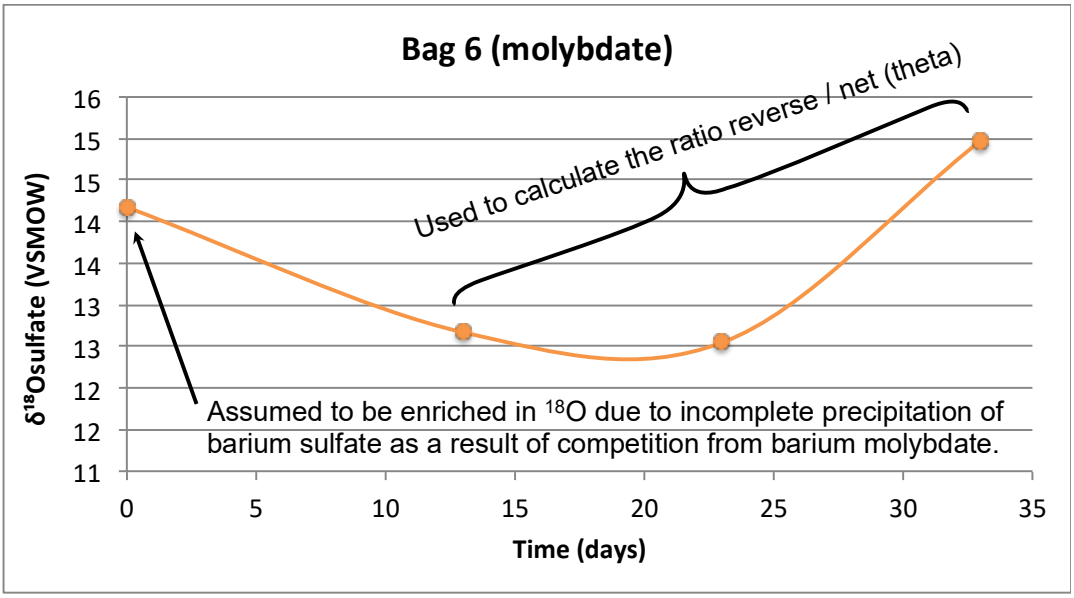

Figure 11. Oxygen isotope results for incubation series 2.
(a) Oxygen isotope trends in incubation series 2 for all incubation bags. (b) A plot of δ^{18}Osulfate against time in the molybdate experiment. A different scale has been used.

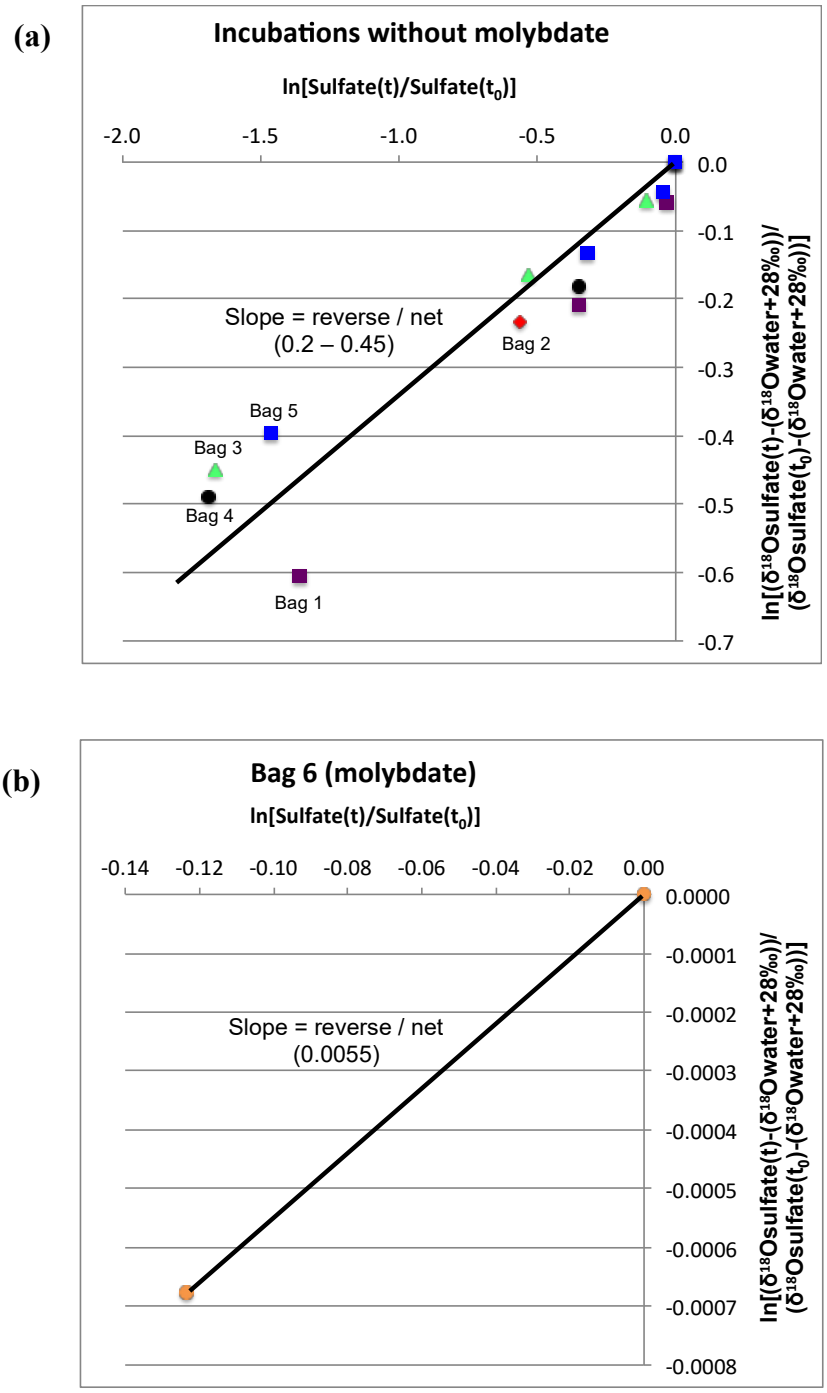

Figure 12. Relationship between oxygen isotope exchange and sulfate reduction rate.
(a) Incubations conducted without molybdate, (b) molybdate experiment. Values plotted on the x-axis correspond the natural logarithm of the remaining fraction of sulfate in the experiments. Values plotted on the y-axis correspond to the natural logarithm of the ratio between the difference of the oxygen isotope composition of sulfate at a chosen time point and the oxygen isotope composition of water, and the difference of the oxygen isotope composition of sulfate at the starting time point and the oxygen isotope composition of water. The slope of the regression line corresponds to Theta (Brunner et al. 2005, Brunner et al. 2012).

REFERENCES

Aharon P. and Fu B. (2000) Microbial sulfate reduction rates and sulfur and oxygen isotope fractionations at oil and gas seeps in deepwater Gulf of Mexico. *Geochim. Cosmochim. Acta* **64**, 233–246.

Aharon P. and Fu B. (2003) Sulfur and oxygen isotopes of coeval sulfate–sulfide in pore fluids of cold seep sediments with sharp redox gradients. *Chem. Geol.* **195**, 201–218.

Bao H. (2006) Purifying Barite for Oxygen Isotope Measurement by Dissolution and Reprecipitation in a Chelating Solution. *Anal. Chem.* **78**, 304–309.

Böttcher M. E., Bernasconi S. M. and Brumsack H.-J. (1999) Carbon, sulfur, and oxygen isotope geochemistry of interstitial waters from the western mediterranean. In *Proceedings of the Ocean Drilling Program, Scientific Results* (eds. R. Zahn, M. C. Comas, and A. Klaus). Ocean Drilling Program, College Station, TX. pp. 413–421.

Böttcher M. E., Brumsack H.-J. and de Lange G. J. (1998) Sulfate reduction and related stable isotope (34S, 18O) variations in interstitial waters from the eastern mediterranean. In *Proceedings of the Ocean Drilling Program, Scientific Results* (eds. A. H. F. Robertson, K.-C. Emeis, C. Richter, and A. Camerlenghi). Ocean Drilling Program, College Station, TX. pp. 365–373.

Böttcher M. E. and Thamdrup B. (2001) Anaerobic sulfide oxidation and stable isotope fractionation associated with bacterial sulfur disproportionation in the presence of MnO2. *Geochim. Cosmochim. Acta* **65**, 1573–1581.

Böttcher M. E., Thamdrup B. and Vennemann T. W. (2001) Oxygen and sulfur isotope fractionation during anaerobic bacterial disproportionation of elemental sulfur. *Geochim. Cosmochim. Acta* **65**, 1601–1609.

Brunner B., Arnold G. L., Røy H., Müller I. A. and Jørgensen B. B. (2016) Off Limits: Sulfate below the Sulfate-Methane Transition. *Front. Earth Sci.* **4**. Available at: http://journal.frontiersin.org/article/10.3389/feart.2016.00075/abstract.

Brunner B. and Bernasconi S. M. (2005) A revised isotope fractionation model for dissimilatory sulfate reduction in sulfate reducing bacteria. *Geochim. Cosmochim. Acta* **69**, 4759–4771.

Brunner B., Bernasconi S. M., Kleikemper J. and Schroth M. H. (2005) A model for oxygen and sulfur isotope fractionation in sulfate during bacterial sulfate reduction processes. *Geochim. Cosmochim. Acta* **69**, 4773–4785.

Brunner B., Einsiedl F., Arnold G. L., Müller I., Templer S. and Bernasconi S. M. (2012) The reversibility of dissimilatory sulphate reduction and the cell-internal multi-step reduction of sulphite to sulphide: insights from the oxygen isotope composition of sulphate. *Isotopes Environ. Health Stud.* **48**, 33–54.

Canfield D. E., Stewart F. J., Thamdrup B., Brabandere L. D., Dalsgaard T., Delong E. F., Revsbech N. P. and Ulloa O. (2010) A Cryptic Sulfur Cycle in Oxygen-Minimum–Zone Waters off the Chilean Coast. *Science* **330**, 1375–1378.

Carlson H. K., Stoeva M. K., Justice N. B., Sczesnak A., Mullan M. R., Mosqueda L. A., Kuehl J. V., Deutschbauer A. M., Arkin A. P. and Coates J. D. (2015) Monofluorophosphate Is a Selective Inhibitor of Respiratory Sulfate-Reducing Microorganisms. *Environ. Sci. Technol.* **49**, 3727–3736.

Deusner C., Holler T., Arnold G. L., Bernasconi S. M., Formolo M. J. and Brunner B. (2014) Sulfur and oxygen isotope fractionation during sulfate reduction coupled to anaerobic oxidation of methane is dependent on methane concentration. *Earth Planet. Sci. Lett.* **399**, 61–73.

Farquhar J., Canfield D. E., Masterson A., Bao H. and Johnston D. (2008) Sulfur and oxygen isotope study of sulfate reduction in experiments with natural populations from Fællestrand, Denmark. *Geochim. Cosmochim. Acta* **72**, 2805–2821.

Fritz P., Basharmal G. M., Drimmie R. J., Ibsen J. and Qureshi R. M. (1989) Oxygen isotope exchange between sulphate and water during bacterial reduction of sulphate. *Chem. Geol. Isot Geosci Sect* **79**, 99–105.

Habashi F. and Bauer E. L. (1966) Aqueous Oxidation of Elemental Sulfur. *Ind. Eng. Chem. Fundam.* **5**, 469–471.

Habicht K. S. and Canfield D. E. (1997) Sulfur isotope fractionation during bacterial sulfate reduction in organic-rich sediments. *Geochim. Cosmochim. Acta* **61**, 5351–5361.

Holmkvist L., Ferdelman T. G. and Jørgensen B. B. (2011) A cryptic sulfur cycle driven by iron in the methane zone of marine sediment (Aarhus Bay, Denmark). *Geochim. Cosmochim. Acta* **75**, 3581–3599.

Holmkvist L., Kamyshny Jr. A., Vogt C., Vamvakopoulos K., Ferdelman T. G. and Jørgensen B. B. (2011) Sulfate reduction below the sulfate–methane transition in Black Sea sediments. *Deep Sea Res. Part Oceanogr. Res. Pap.* **58**, 493–504.

Jasińska A., Burska D. and Bolałek J. (2012) Sulfur in the marine environment. *Oceanol. Hydrobiol. Stud.* **41**, 72–82.

Ku T. C. W., Walter L. M., Coleman M. L., Blake R. E. and Martini A. M. (1999) Coupling between sulfur recycling and syndepositional carbonate dissolution: evidence from oxygen and sulfur isotope composition of pore water sulfate, South Florida Platform, U.S.A. *Geochim. Cosmochim. Acta* **63**, 2529–2546.

Leloup J., Fossing H., Kohls K., Holmkvist L., Borowski C. and Jørgensen B. B. (2009) Sulfate-reducing bacteria in marine sediment (Aarhus Bay, Denmark): abundance and diversity related to geochemical zonation. *Environ. Microbiol.* **11**, 1278–1291.

Leloup J., Loy A., Knab N. J., Borowski C., Wagner M. and Jørgensen B. B. (2007) Diversity and abundance of sulfate-reducing microorganisms in the sulfate and methane zones of a marine sediment, Black Sea. *Environ. Microbiol.* **9**, 131–142.

Milucka J., Ferdelman T. G., Polerecky L., Franzke D., Wegener G., Schmid M., Lieberwirth I., Wagner M., Widdel F. and Kuypers M. M. M. (2012) Zero-valent sulphur is a key intermediate in marine methane oxidation. *Nature* **491**, 541–546.

Mizutani Y. and Rafter T. A. (1969) Oxygen Isotopic Composition of Sulphates. Part 4. Bacterial Fractionation of Oxygen Isotopes in the Reduction of Sulphate and in the Oxidation of Sulphur. *N Z J Sci 12 60-8Mar 1969*. Available at: https://www.osti.gov/scitech/biblio/4764537.

Müller I. A., Brunner B. and Coleman M. (2013) Isotopic evidence of the pivotal role of sulfite oxidation in shaping the oxygen isotope signature of sulfate. *Chem. Geol.* **354**, 186–202.

Rees C. E. (1973) A steady-state model for sulphur isotope fractionation in bacterial reduction processes. *Geochim. Cosmochim. Acta* **37**, 1141–1162.

Scheller S., Yu H., Chadwick G. L., McGlynn S. E. and Orphan V. J. (2016) Artificial electron acceptors decouple archaeal methane oxidation from sulfate reduction. *Science* **351**, 703–707.

Wing B. A. and Halevy I. (2014) Intracellular metabolite levels shape sulfur isotope fractionation during microbial sulfate respiration. *Proc. Natl. Acad. Sci.* **111**, 18116–18125.

Zeebe R. E. (2010) A new value for the stable oxygen isotope fractionation between dissolved sulfate ion and water. *Geochim. Cosmochim. Acta* **74**, 818–828.

VITA

Kamurugu, a small village in rural Kenya. This is where Michael Ngari Mathuri was born. Like many other rural kids, Mathuri was raised by his grandmother. His mother who was the sole breadwinner for the family was working in the Kenyan capital, Nairobi.

Upon graduating from High School, Michael Ngari Mathuri was admitted to Kenyatta University in Kenya where he studied a Bachelor of Science Degree majoring in Biochemistry. Immediately after his graduation in December 2013 his former professor at the university employed him as a research assistant, a position he held until May 2015. It is during this period that Michael Ngari Mathuri fell in love with microbes.

Following his interests in geomicrobiology, in the Summer of 2015 Michael Ngari Mathuri moved to El Paso, Texas to pursue his Master of Science Degree in Geological Sciences at the University of Texas at El Paso (UTEP). During his time at UTEP he was an active member of American Association of Petroleum Geologists (AAPG) and Center for Entrepreneurial Geosciences (CEGS).

After completing his Master's Degree, Michael Ngari Mathuri will move to Connecticut where he will join the Ph.D. Program in Oceanography at the University of Connecticut (UConn) to further his science research in marine environments.

Email: mykmathuri@gmail.com

This thesis was typed by the author, Michael Ngari Mathuri.